

Theoretical Investigation of Functional Responses of Bio-molecular Assembly Networks

Pankaj Gautam¹, and Sudipta Kumar Sinha^{1*}

¹*Theoretical and Computational Biophysical Chemistry Group, Department of Chemistry, Indian Institute of Technology Ropar, Rupnagar, Punjab - 140001, India*

I. THE GRAND PARTITION FUNCTION

Various protein-protein and protein-DNA interactions are the central to the formation of Transcription Activation Complex (TAC), and these interactions can be quantified by several parameters those are tunable by the selection and placement of various protein binding DNA sequences. Here, we employ equilibrium statistical mechanics and explore the cooperative effects for calculating the binding probability of various TACs formed on DNA for these intricate network motifs. These complexes are the results of combinations of various bio-molecules such as RNA polymerase(R), transcription factor(P), and signaling molecule(s). As stated in the main text that the central theme in this problem is the calculation of population of various complexes formed for different network motifs under grand canonical ensemble at thermodynamic equilibrium. We present the theoretical calculations in detail to obtain fractions of transcription active complexes (TAC) and its function, fold change(FC) for few well known network motifs ranging from simple activation/repression, feedback (FBL) to feed forward (FFL) loops. The detailed derivation for the calculation of fraction or FC for various complexes can be found elsewhere[1, 2]. The general framework of our theory is described in the main paper. Here, we describe the few specific protein-DNA interaction networks below.

Activation ($X \rightarrow Y$) and Repression ($X \dashv Y$)

As mentioned in the main paper, we consider a gene regulatory network that consists of a regulatory gene G_X and a structural gene G_Y , and explore the activation or repression of G_Y by G_X . The gene product of G_X is TF_Y that can act either as an activator or a repressor to the gene G_Y and produces its desired output. Let R_X and R_Y bind to the G_X and G_Y respectively and their respective site partition functions are q_{R_X} and q_{R_Y} . To define the grand partition function for the activation and repression, we consider that TF_Y acts as an activator for G_Y , and its free energy of interactions with bound RNAP (R_Y) is $\epsilon_{R_Y Y}$. Therefore, we can write the grand canonical partition function for the network of biomolecular interactions for a system composed of M identical units is given by $\Xi = \xi^M$. As given in the main text, $\Xi(\lambda, M, T) = (\xi_{OFF} + \xi_{ON})^M$. The partition function ξ for an unit can be decomposed into ON and OFF based on their microstates, hence we write $\xi = \xi_{OFF} + \xi_{ON}$, where $\xi_{OFF} = 1 + q_{R_X} \lambda_{R_X} (1 + q_Y \lambda_Y)$ and $\xi_{ON} = q_{R_Y} \lambda_{R_Y} + q_{R_X} \lambda_{R_X} q_{R_Y} \lambda_{R_Y} (1 + q_Y \lambda_Y e^{-\frac{\epsilon_{R_Y Y}}{k_B T}})$.

Notice that the binding of R_Y happen only through a coordinated interactions among all the components present in the network, and hence it also defines the population of TACs present in the system. Therefore, we can calculate the fraction bound RNAP to the G_Y gene ($o_{\bar{R}_Y}$) as a response function of the network, can be obtained by the following manner, $o_{\bar{R}_Y} = \frac{\lambda_{R_Y}}{M} \left(\frac{\partial \ln \Xi}{\partial \lambda_{R_Y}} \right)_{M, T}$

$$o_a = o_{\bar{R}_Y} = \frac{\xi_{ON}}{\xi} \quad (S1)$$

Here the term $\omega = e^{-\frac{\epsilon_{R_Y Y}}{k_B T}}$ is the pairwise cooperative factor between $RNAP$ and TFs . If the value of $\omega > 1$, there is a favourable free energy of interaction between $RNAP$ and TFs that enhances the recruitment of $RNAP$ by a bound TF . There are two ways where two proteins bind cooperatively if they bound to adjacent sites or if they can contact through DNA looping. The DNA looping further modulates the ω at least by a factor of 5 as compared to the ω for nearest neighbor interactions. If the value of $\omega = 0$, there is a mutual exclusion between two proteins when their binding sites are made to overlap. We exploit this particular condition to model the TF as a repressor. The

* To whom correspondence should be addressed. Tel: +91 (0)1881-23-2066; Email: sudipta@iitpr.ac.in

value of $\omega = 1$ corresponds to both of the *RNAP* and *TF* bind independently and the mutual interaction between them is turned off. Both of the *RNAP* and *TF* are well separated on the DNA under this condition.

Similar to the activation, the repression effect can be defined as the unbinding of R_Y from the DNA. Once again we exploit the protein-DNA and protein-protein interactions for repression. We show that a favourable binding between TF and DNA and unfavourable binding between RNAP and TF introduces a competition between TF and RNAP for the binding with DNA. Therefore, we tune the cooperative factor by setting a condition $\omega = 0$ on ξ_{ON} i.e. mutually exclusive interactions for the repression. It calculates the fraction of unbound RNAP from G_Y , (o_{R_Y}) Thus the repression is defined as $o_{R_Y} = [\frac{\xi_{ON}}{\xi}]_{\omega=0} = q_{R_Y} \lambda_{R_Y} + q_{R_X} \lambda_{R_X} q_{R_Y} \lambda_{R_Y}$. However in many instances, the repression can also be defined as the binding of the repressor to G_Y , which is nothing but the $o_r = 1 - o_{R_Y} = 1 - \frac{\xi_{ON}}{\xi} = \frac{\xi_{OFF}}{\xi}$.

Induced activation ($X \rightarrow Y \leftarrow s_Y$) and Induced repression ($X \dashv Y \leftarrow s_Y$):

Since the binding of a signalling molecule to the TF modulates the interaction between DNA and TF, it can alter the population of active complexes. Here, we show how the strength of the interaction between *TF* and signalling molecule affect the population of TACs. The problem is very similar to the previous one but two additional components are introduced here. Such increments in components increases the number of microstates of the network that further affects the population of the TACs. Let s_Y represents the signaling molecule that interacts with TF_Y with ϵ_{s_Y} interaction energy and this TF_Y is an activator for G_Y , thus there exist $\epsilon_{R_Y Y}$ interaction energy between R_Y and TF_Y . So, we can write the grand canonical partition function for M sites as $\Xi = \xi^M$. The function ξ for this system is $\xi = \xi_{OFF} + \xi_{ON}$, where $\xi_{OFF} = 1 + q_{R_X} \lambda_{R_X} (1 + q_Y \lambda_Y (1 + q_{s_Y} \lambda_{s_Y} e^{-\frac{\epsilon_{s_Y}}{k_B T}}))$ and $\xi_{ON} = q_{R_Y} \lambda_{R_Y} (1 + q_{R_X} \lambda_{R_X} (1 + q_Y \lambda_Y (1 + q_{s_Y} \lambda_{s_Y} e^{-\frac{\epsilon_{s_Y}}{k_B T}}) e^{-\frac{\epsilon_{R_Y Y}}{k_B T}}))$. Therefore, we can calculate the fraction bound RNAP to the G_Y (o_{R_Y}) as $o_{R_Y} = \frac{\lambda_{R_Y}}{M} \left(\frac{\partial \ln \Xi}{\partial \lambda_{R_Y}} \right)_{M,T}$

$$o_{R_Y} = \frac{\xi_{ON}}{\xi} \quad (S2)$$

Similar to the simple repression, the TF_Y is a repressor. We consider signaling species, s_Y interacts with TF_Y with ϵ_{s_Y} interaction energy and this TF_Y acts as a repressor for G_Y . Here we include the repression effect by considering the excluded volume interaction of TF_Y and R_Y , which prevents binding mutually one another. Therefore, we can calculate the fraction of unbound R_Y due to the binding of TF_Y to the G_Y (o_{R_Y}) is given by, $o_{R_Y} = [\frac{\xi_{ON}}{\xi}]_{\omega=0}$, where the ξ_{ON} is defined as $q_{R_Y} \lambda_{R_Y} + q_{R_X} \lambda_{R_X} q_{R_Y} \lambda_{R_Y}$. However, one can also define the repression in terms of the binding of bound repressor to the G_Y , which is nothing but the $o_r = 1 - o_{R_Y} = 1 - \frac{\xi_{ON}}{\xi} = \frac{\xi_{OFF}}{\xi}$.

Higher Order Protein-DNA Interaction Networks

The above activation and repression can be combined together that creates a programmable complex assemblies that control the higher order mechanisms. Out of them feedback and feedforward loops are common and we present their thermodynamic formalism here. The general framework for this calculation is to define the grand canonical partition function for the protein-DNA interaction networks and then explore their overall responses in terms of the binding/unbinding of the RNAP molecule to a particular gene. We show that our proposed thermodynamic formalism works well for these higher order protein-DNA interaction networks.

Feedback Loops

In case of FBL, we consider that TF_Y which is a genetic product of G_X acts as either an activator or repressor for G_Y and TF_X which is a genetic product of G_Y acts as either an activator or repressor for G_X and thus there exist $\epsilon_{R_Y Y}, \epsilon_{R_X X}$ interaction energy between R_Y - TF_Y and R_X - TF_X respectively. Suppose s_X and s_Y represent the signaling species which interacts with TF_X and TF_Y with ϵ_{s_X} and ϵ_{s_Y} interaction energies respectively. So, we can write the grand canonical partition function, $\Xi = \xi^M$ for this case.

The function ξ for FBL is $\xi = \xi_{OFF} + \xi_{ON}$, where $\xi_{OFF} = 1 + q_{R_Y} \lambda_{R_Y} (1 + q_X \lambda_X (1 + q_{s_X} \lambda_{s_X} e^{-\frac{\epsilon_{s_X}}{k_B T}}))$, and $\xi_{ON} = q_{R_X} \lambda_{R_X} (1 + q_{R_Y} \lambda_{R_Y} (1 + q_X \lambda_X e^{-\frac{\epsilon_{R_X X}}{k_B T}} (1 + q_{s_X} \lambda_{s_X} e^{-\frac{\epsilon_{s_X}}{k_B T}}) + q_Y \lambda_Y e^{-\frac{\epsilon_{R_Y Y}}{k_B T}} (1 + q_{s_Y} \lambda_{s_Y} e^{-\frac{\epsilon_{s_Y}}{k_B T}}) +$

$q_Y \lambda_Y q_X \lambda_X e^{-\frac{\epsilon_{R_Y Y}}{k_B T}} e^{-\frac{\epsilon_{R_X X}}{k_B T}} (1 + q_{s_Y} \lambda_{s_Y} e^{-\frac{\epsilon_{s_Y}}{k_B T}}) (1 + q_{s_X} \lambda_{s_X} e^{-\frac{\epsilon_{s_X}}{k_B T}}) + q_Y \lambda_Y (1 + q_{s_Y} \lambda_{s_Y} e^{-\frac{\epsilon_{s_Y}}{k_B T}})$. Therefore, we can calculate the fraction($o_{\bar{R}_X}$) of structural R_X that has bound to DNA $o_{\bar{R}_X} = \frac{\lambda_{R_X}}{M} \left(\frac{\partial \ln \Xi}{\partial \lambda_{R_X}} \right)_{M,T}$

$$o_{\bar{R}_X} = \frac{1}{\xi} (q_{R_X} \lambda_{R_X} (1 + q_{R_Y} \lambda_{R_Y} (1 + q_X \lambda_X e^{-\frac{\epsilon_{R_X X}}{k_B T}} (1 + q_{s_X} \lambda_{s_X} e^{-\frac{\epsilon_{s_X}}{k_B T}}) + q_Y \lambda_Y e^{-\frac{\epsilon_{R_Y Y}}{k_B T}} (1 + q_{s_Y} \lambda_{s_Y} e^{-\frac{\epsilon_{s_Y}}{k_B T}}) + q_Y \lambda_Y q_X \lambda_X e^{-\frac{\epsilon_{R_Y Y}}{k_B T}} e^{-\frac{\epsilon_{R_X X}}{k_B T}} (1 + q_{s_Y} \lambda_{s_Y} e^{-\frac{\epsilon_{s_Y}}{k_B T}}) (1 + q_{s_X} \lambda_{s_X} e^{-\frac{\epsilon_{s_X}}{k_B T}}) + q_Y \lambda_Y (1 + q_{s_Y} \lambda_{s_Y} e^{-\frac{\epsilon_{s_Y}}{k_B T}}))) \quad (S3)$$

Also, we can calculate the fraction($o_{\bar{R}_Y}$) of structural R_Y that has bound to DNA $o_{\bar{R}_Y} = \frac{\lambda_{R_Y}}{M} \left(\frac{\partial \ln \Xi}{\partial \lambda_{R_Y}} \right)_{M,T}$

$$o_{\bar{R}_Y} = \frac{1}{\xi} (q_{R_Y} \lambda_{R_Y} (1 + q_{R_X} \lambda_{R_X} (1 + q_Y \lambda_Y w_{R_Y} (1 + q_{s_Y} \lambda_{s_Y} e^{-\frac{\epsilon_{s_Y}}{k_B T}}) + q_X \lambda_X e^{-\frac{\epsilon_{R_X X}}{k_B T}} (1 + q_{s_X} \lambda_{s_X} e^{-\frac{\epsilon_{s_X}}{k_B T}}) + q_Y \lambda_Y q_X \lambda_X e^{-\frac{\epsilon_{R_Y Y}}{k_B T}} e^{-\frac{\epsilon_{R_X X}}{k_B T}} (1 + q_{s_Y} \lambda_{s_Y} e^{-\frac{\epsilon_{s_Y}}{k_B T}}) (1 + q_{s_X} \lambda_{s_X} e^{-\frac{\epsilon_{s_X}}{k_B T}}) + q_X \lambda_X (1 + q_{s_X} \lambda_{s_X} e^{-\frac{\epsilon_{s_X}}{k_B T}}))) \quad (S4)$$

A. Feedforward Loops

In case of FFL, we consider that TF_Y which is a gene product of G_X that acts either as an activator or a repressor for G_Y and G_A . Also, the gene product of G_Y is TF_A which acts as either an activator or repressor for G_A and thus there exist $\epsilon_{R_Y Y}, \epsilon_{R_A Y}$ and $\epsilon_{R_A A}$ interaction energy between R_Y-TF_Y, R_A-TF_Y and R_A-TF_A respectively. Suppose s_Y and s_A represent the signaling species which interacts with TF_Y and TF_A with ϵ_{s_Y} and ϵ_{s_A} interaction energies respectively. Now, as given in the main text there exist a total of eight possible configurations depending on the binding of TF_Y and TF_A to their respective promoter regions. So, we can write the grand canonical partition function, $\Xi = \xi^M$ for the FFL network motif.

The function ξ for G_A is $\xi = \xi_{OFF} + \xi_{ON}$, where $\xi_{OFF} = 1 + \xi_{OFF_1} + \xi_{OFF_2} + \xi_{OFF_3} + \xi_{OFF_4}$, and $\xi_{ON} = \xi_{ON_1} + \xi_{ON_2} + \xi_{ON_3} + \xi_{ON_4}$, where

$$\xi_{OFF_1} = q_{R_Y} \lambda_{R_Y} (1 + q_A \lambda_A (1 + q_{s_A} \lambda_{s_A})) + q_{R_X} \lambda_{R_X} (1 + q_Y^A \lambda_Y (1 + q_{s_Y}^A \lambda_{s_Y})) + q_{R_X} \lambda_{R_X} q_{R_Y} \lambda_{R_Y} (1 + q_A \lambda_A (1 + q_{s_A} \lambda_{s_A}) + q_Y^A \lambda_Y),$$

$$\xi_{OFF_2} = q_{R_X} \lambda_{R_X} (q_{s_Y} \lambda_{s_Y} (1 + q_Y^A \lambda_Y (1 + q_{s_Y}^A \lambda_{s_Y})) + q_{R_Y} \lambda_{R_Y} (q_Y \lambda_Y w_{R_Y} (1 + q_A \lambda_A) + q_Y^A \lambda_Y (q_A \lambda_A (1 + q_{s_A} \lambda_{s_A}) + q_{s_Y}^A \lambda_{s_Y} (1 + q_A \lambda_A (1 + q_{s_A} \lambda_{s_A}))))),$$

$$\xi_{OFF_3} = q_{R_X} \lambda_{R_X} (q_Y \lambda_Y q_{s_Y} \lambda_{s_Y} (1 + q_Y^A \lambda_Y (1 + q_{s_Y}^A \lambda_{s_Y})) + q_{R_Y} \lambda_{R_Y} q_Y \lambda_Y (q_A \lambda_A q_{s_A} \lambda_{s_A} w_{R_Y} + q_Y^A \lambda_Y q_{s_Y}^A \lambda_{s_Y} w_{R_Y} (1 + q_A \lambda_A (1 + q_{s_A} \lambda_{s_A})) + q_Y^A \lambda_Y w_{R_Y} (1 + q_A \lambda_A (1 + q_{s_A} \lambda_{s_A})))),$$

$$\xi_{OFF_4} = q_{R_X} \lambda_{R_X} q_{R_Y} \lambda_{R_Y} q_Y \lambda_Y q_{s_Y} \lambda_{s_Y} w_{R_Y} (1 + q_A \lambda_A (1 + q_{s_A} \lambda_{s_A}) + q_Y^A \lambda_Y (1 + q_{s_Y}^A \lambda_{s_Y}) + q_{s_A} \lambda_{s_A} (1 + q_{s_Y}^A \lambda_{s_Y})) + q_Y^A \lambda_Y (1 + q_{s_Y}^A \lambda_{s_Y}),$$

$$\xi_{ON_1} = q_{R_A} \lambda_{R_A} (1 + q_{R_Y} \lambda_{R_Y} (1 + q_A \lambda_A w_{R_A} (1 + q_{s_A} \lambda_{s_A})) + q_{R_X} \lambda_{R_X} (1 + q_Y^A \lambda_Y w_{R_A}^A (1 + q_{s_Y}^A \lambda_{s_Y}) + q_{R_Y} \lambda_{R_Y} (1 + q_A \lambda_A w_{R_A} (1 + q_{s_A} \lambda_{s_A}))))),$$

$$\xi_{ON_2} = q_{R_A} \lambda_{R_A} q_{R_X} \lambda_{R_X} (q_Y \lambda_Y (1 + q_Y^A \lambda_Y w_{R_A}^A (1 + q_{s_Y}^A \lambda_{s_Y})) + q_{R_Y} \lambda_{R_Y} (q_Y \lambda_Y w_{R_Y} + q_Y^A \lambda_Y w_{R_A}^A (1 + q_A \lambda_A w_{R_A} (1 + q_{s_A} \lambda_{s_A})) + q_{s_Y}^A \lambda_{s_Y} (1 + q_A \lambda_A w_{R_A} (1 + q_{s_A} \lambda_{s_A}))))),$$

$$\xi_{ON_3} = q_{R_A} \lambda_{R_A} q_{R_X} \lambda_{R_X} q_Y \lambda_Y (q_{s_Y} \lambda_{s_Y} (1 + q_Y^A \lambda_Y w_{R_A}^A) + q_{R_Y} \lambda_{R_Y} (q_A \lambda_A w_{R_Y} w_{R_A} (1 + q_{s_A} \lambda_{s_A}) + q_Y^A \lambda_Y w_{R_Y} w_{R_A} (1 + q_A \lambda_A w_{R_A} (1 + q_{s_A} \lambda_{s_A})) + q_{s_Y}^A \lambda_{s_Y} (1 + q_A \lambda_A w_{R_A} (1 + q_{s_A} \lambda_{s_A}))))),$$

$$\xi_{ON_4} = q_{R_A} \lambda_{R_A} q_{R_X} \lambda_{R_X} q_Y \lambda_Y q_{s_Y} \lambda_{s_Y} (q_Y^A \lambda_Y q_{s_Y}^A \lambda_{s_Y} w_{R_A}^A + q_{R_Y} \lambda_{R_Y} w_{R_Y} (1 + q_A \lambda_A w_{R_A} (1 + q_{s_A} \lambda_{s_A}) + q_Y^A \lambda_Y w_{R_A}^A (1 + q_A \lambda_A w_{R_A} (1 + q_{s_A} \lambda_{s_A})) + q_{s_Y}^A \lambda_{s_Y} (1 + q_A \lambda_A w_{R_A} (1 + q_{s_A} \lambda_{s_A}))))),$$

Therefore, we can calculate the fraction($o_{\bar{R}_A}$) of structural R_A that has bound to DNA $o_{\bar{R}_A} = \frac{\lambda_{R_A}}{M} \left(\frac{\partial \ln \Xi}{\partial \lambda_{R_A}} \right)_{M,T}$

$$o_{\bar{R}_A} = \frac{\xi_{ON}}{\xi} \quad (S5)$$

II. DYNAMICS

We also develop a dynamical model for the activation, repression, FL, and FFL Network motifs. We assumed that the promoter corresponding to X, Y, and A genes switch between two states, i.e., G_i , and G_i^* , where $i \in (X, Y, A)$. Here, G_i is associated with the basal expression(i.e., only RNAP is bound to the promoter) and G_i^* is presenting the stimulated expression(i.e., RNAP is present along with either an activator and repressor). Also, every state corresponds to a different protein production rate. The binding of protein is responsible for switching between G_i and G_i^* . Furthermore, the protein molecule itself can undergo a transition from a normal state, i.e., P_i , and an induced state, i.e., P_i^* with the aid of ligand molecule L_i . In general, we consider four types of elementary reactions, a) basal expression that happens upon binding of only RNAP, b) activation of promoter state happens upon forming a complex with TFs, c) controlled gene expression mediated through RNAP-TF interactions, and d) degradation of proteins in our modeling scheme. Thus, the various reactions for the stochastic simulation for these network motifs and corresponding deterministic equations are presented as follows.

A. Activation and Repression

TABLE S1: This table contains various elementary reactions for the activation(A), repression(R), Induced activation(IA), Induced repression(IR) network motifs. Here, G_X and G_Y represent the genes with the basal expression, G_Y^* represents the activated gene, and G_Y^\ominus represents the repressed gene. Also, TF_X and TF_Y represent the proteins that are expressed by G_X and G_Y , respectively. The specific reaction rates for each reaction are shown on the marked arrows.

A	R	IA	IR
1) $G_X \xrightarrow{\rho_X} G_X + TF_X$	1) $G_X \xrightarrow{\rho_X} G_X + TF_X$	1) $G_X \xrightarrow{\rho_X} G_X + TF_X$	1) $G_X \xrightarrow{\rho_X} G_X + TF_X$
2) $G_Y \xrightarrow{\rho_Y} G_Y + TF_Y$	2) $G_Y \xrightarrow{\rho_Y} G_Y + TF_Y$	2) $G_Y \xrightarrow{\rho_Y} G_Y + TF_Y$	2) $G_Y \xrightarrow{\rho_Y} G_Y + TF_Y$
3) $G_Y + TF_X \xrightarrow{\sigma_{PYX}} G_Y^*$	3) $G_Y + TF_X \xrightarrow{\kappa_{YY}} G_Y^\ominus$	3) $TF_X + L_X \xrightarrow{\sigma_X} TF_X^*$	3) $TF_X + L_X \xrightarrow{\sigma_X} TF_X^*$
4) $G_Y^* \xrightarrow{\sigma_{PYX'}} G_Y + TF_X$	4) $G_Y^\ominus \xrightarrow{\kappa_{YY'}} G_Y + TF_X$	4) $TF_X^* \xrightarrow{\sigma_X'} TF_X + L_X$	4) $TF_X^* \xrightarrow{\sigma_X'} TF_X + L_X$
5) $G_Y^* \xrightarrow{\rho_{YY'}} G_Y^* + TF_Y$	5) $TF_X \xrightarrow{k_{dX}} \phi$	5) $G_Y + TF_X^* \xrightarrow{\sigma_{PY}} G_Y^*$	5) $G_Y + TF_X^* \xrightarrow{\kappa_Y} G_Y^\ominus$
6) $TF_X \xrightarrow{k_{dX}} \phi$	6) $TF_Y \xrightarrow{k_{dY}} \phi$	6) $G_Y^* \xrightarrow{\sigma_{PY'}} G_Y + TF_X^*$	6) $G_Y^\ominus \xrightarrow{\kappa_Y'} G_Y + TF_X^*$
7) $TF_Y \xrightarrow{k_{dY}} \phi$		7) $G_Y^* \xrightarrow{\rho_Y'} G_Y^* + TF_Y$	7) $TF_X \xrightarrow{k_{dX}} \phi$
		8) $TF_X \xrightarrow{k_{dX}} \phi$	8) $TF_Y \xrightarrow{k_{dY}} \phi$
		9) $TF_Y \xrightarrow{k_{dY}} \phi$	

The x vector corresponding to equation 6 in the main paper that is associated with the reaction network for activation is $x = [G_Y \ G_Y^* \ TF_X \ TF_Y]'$ and stoichiometry matrix S for the same is given as follows

$$S_A = \begin{pmatrix} 0 & 0 & -1 & 1 & 0 & 0 & 0 \\ 0 & 0 & 1 & -1 & 0 & 0 & 0 \\ 1 & 0 & -1 & 1 & 0 & -1 & 0 \\ 0 & 1 & 0 & 0 & 1 & 0 & -1 \end{pmatrix}$$

Also, $F(X)$ is written as $[\rho_X G_X \ \rho_Y G_Y \ \sigma_{PYX} G_Y TF_X \ \sigma_{PYX'} G_Y^* \ \rho_{YY'} G_Y^* \ k_{dX} TF_X \ k_{dY} TF_Y]'$

The x vector associated with the reaction network for repression is $x = [G_Y \ G_Y^\ominus \ TF_X \ TF_Y]'$ and stoichiometry matrix S for the same is given as follows

$$S_R = \begin{pmatrix} 0 & 0 & -1 & 1 & 0 & 0 \\ 0 & 0 & 1 & -1 & 0 & 0 \\ 1 & 0 & -1 & 1 & -1 & 0 \\ 0 & 1 & 0 & 0 & 0 & -1 \end{pmatrix}$$

Also, $F(X)$ is written as $[\rho_X G_X \ \rho_Y G_Y \ \kappa_{YY} G_Y TF_X \ \kappa_{YY'} G_Y^\ominus \ k_{dX} TF_X \ k_{dY} TF_Y]'$

The x vector associated with the reaction network for Induced activation is $x = [G_Y G_Y^* TF_X L_X TF_X^* TF_Y]'$ and stoichiometry matrix S for the same is given as follows

$$S_{IA} = \begin{pmatrix} 0 & 0 & 0 & 0 & -1 & 1 & 0 & 0 & 0 \\ 0 & 0 & 0 & 0 & 1 & -1 & 0 & 0 & 0 \\ 1 & 0 & -1 & 1 & 0 & 0 & 0 & -1 & 0 \\ 0 & 0 & -1 & 1 & 0 & 0 & 0 & 0 & 0 \\ 0 & 0 & 1 & -1 & -1 & 1 & 0 & 0 & 0 \\ 0 & 1 & 0 & 0 & 0 & 0 & 1 & 0 & -1 \end{pmatrix}$$

Also, $F(X)$ is written as $[\rho_X G_X \rho_Y G_Y \sigma_X TF_X L_X \sigma_X' TF_X^* \sigma_{PY} G_Y TF_X^* \sigma_{PY}' G_Y^* \rho_Y' G_Y^* k_{dX} TF_X k_{dY} TF_Y]'$
 The x vector associated with the reaction network for induced repression is, $x = [G_Y G_Y^\ominus TF_X L_X TF_X^* TF_Y]'$ and stoichiometry matrix S for the same is given as follows

$$S_{IR} = \begin{pmatrix} 0 & 0 & 0 & 0 & -1 & 1 & 0 & 0 \\ 0 & 0 & 0 & 0 & 1 & -1 & 0 & 0 \\ 1 & 0 & -1 & 1 & 0 & 0 & -1 & 0 \\ 0 & 0 & -1 & 1 & 0 & 0 & 0 & 0 \\ 0 & 0 & 1 & -1 & -1 & 1 & 0 & 0 \\ 0 & 1 & 0 & 0 & 0 & 0 & 0 & -1 \end{pmatrix}$$

Also, $F(X)$ is written as $[\rho_X G_X \rho_Y G_Y \sigma_X TF_X L_X \sigma_X' TF_X^* \kappa_Y G_Y TF_X^* \kappa_Y' G_Y^\ominus k_{dX} TF_X k_{dY} TF_Y]'$

TABLE S2: The deterministic equations for the A, R, IA, and IR network motifs are shown here. We follow the symbols presented in Table S1 to write the rate equations.

A	R
$\frac{dG_Y}{dt} = -\sigma_{P_{YY}}G_YTF_X + \sigma'_{P_{YY}}G_Y^*$	$\frac{dG_Y}{dt} = -\kappa_YG_YTF_X + \kappa'_YG_Y^\ominus$
$\frac{dG_Y^*}{dt} = \sigma_{P_{YY}}G_YTF_X - \sigma'_{P_{YY}}G_Y^*$	$\frac{dG_Y^\ominus}{dt} = \kappa_YG_YTF_X - \kappa'_YG_Y^\ominus$
$\frac{dTF_X}{dt} = \rho_XG_X - \sigma_{P_{YY}}G_YTF_X + \sigma'_{P_{YY}}G_Y^* - k_{dX}TF_X$	$\frac{dTF_X}{dt} = \rho_XG_X - \kappa_YG_YTF_X + \kappa'_YG_Y^\ominus - k_{dX}TF_X$
$\frac{dTF_Y}{dt} = \rho_YG_Y + \rho'_{YY}G_Y^* - k_{dY}TF_Y$	$\frac{dTF_Y}{dt} = \rho_YG_Y - k_{dY}TF_Y$
IA	IR
$\frac{dG_Y}{dt} = -\sigma_{P_Y}G_YTF_X^* + \sigma'_{P_Y}G_Y^*$	$\frac{dG_Y}{dt} = -\kappa_YG_YTF_X^* + \kappa'_YG_Y^\ominus$
$\frac{dG_Y^*}{dt} = \sigma_{P_Y}G_YTF_X^* - \sigma'_{P_Y}G_Y^*$	$\frac{dG_Y^\ominus}{dt} = \kappa_YG_YTF_X^* - \kappa'_YG_Y^\ominus$
$\frac{dTF_X}{dt} = \rho_XG_X - \sigma_XTF_XL_X + \sigma'_XTF_X^* - k_{dX}TF_X$	$\frac{dTF_X}{dt} = \rho_XG_X - \sigma_XTF_XL_X + \sigma'_XTF_X^* - k_{dX}TF_X$
$\frac{dTF_Y}{dt} = \rho_YG_Y + \rho'_Y G_Y^* - k_{dY}TF_Y$	$\frac{dTF_X^*}{dt} = \sigma_XTF_XL_X - \sigma'_XTF_X^* - \kappa_YG_YTF_X^* + \kappa'_YG_Y^\ominus$
$\frac{dTF_X^*}{dt} = \sigma_XTF_XL_X - \sigma'_XTF_X^* - \sigma_{P_Y}G_YTF_X^* + \sigma'_{P_Y}G_Y^*$	$\frac{dTF_Y}{dt} = \rho_YG_Y - k_{dY}TF_Y$
$\frac{dL_X}{dt} = -\sigma_XTF_XL_X + \sigma'_XTF_X^*$	$\frac{dL_X}{dt} = -\sigma_XTF_XL_X + \sigma'_XTF_X^*$

Similar to the activation and repression, the elementary reactions are presented in the following table. Following the same method shown for activation and repression, we can also write the deterministic rate equations for this case. However, the set of equations is quite large and repetitive; we avoid them writing again here. However, we obtain the deterministic and stochastic trajectories by considering those elementary biomolecular reactions as presented in Table S3.

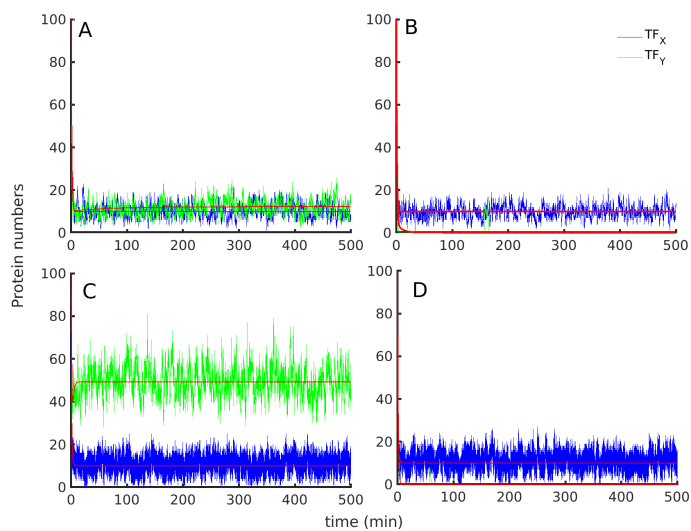


FIG. S1: Trajectories obtained from stochastic simulations are presented. Here panels A, B, C, and D refer to the production of proteins for simple activation, repression, induced activation, and repression, respectively. Here red colored solid lines for all the cases correspond to the deterministic results. A clear correspondence between deterministic and stochastic results is visible in the figure. The parameters associated with these results are given in the table S7.

B. FBL

TABLE S3: Elementary reactions for the FBL network motifs are presented in this table. Here, G_X and G_Y represent the genes with the basal expression, G_X^* and G_Y^* represent the activated genes, and G_X^\ominus and G_Y^\ominus represent the repressed genes. Also, TF_X and TF_Y represent the proteins that are expressed by G_X and G_Y , respectively. The specific reaction rates for each reaction are shown on the marked arrows.

PFL	NFL1	NFL2	FNFL
1) $G_X \xrightarrow{\rho_X} G_X + TF_X$	1) $G_X \xrightarrow{\rho_X} G_X + TF_X$	1) $G_X \xrightarrow{\rho_X} G_X + TF_X$	1) $G_X \xrightarrow{\rho_X} G_X + TF_X$
2) $G_Y \xrightarrow{\rho_Y} G_Y + TF_Y$	2) $G_Y \xrightarrow{\rho_Y} G_Y + TF_Y$	2) $G_Y \xrightarrow{\rho_Y} G_Y + TF_Y$	2) $G_Y \xrightarrow{\rho_Y} G_Y + TF_Y$
3) $TF_X + L_X \xrightarrow{\sigma_X} TF_X^*$	3) $TF_X + L_X \xrightarrow{\sigma_X} TF_X^*$	3) $TF_X + L_X \xrightarrow{\sigma_X} TF_X^*$	3) $TF_X + L_X \xrightarrow{\sigma_X} TF_X^*$
4) $TF_X^* \xrightarrow{\sigma_X'} TF_X + L_X$	4) $TF_X^* \xrightarrow{\sigma_X'} TF_X + L_X$	4) $TF_X^* \xrightarrow{\sigma_X'} TF_X + L_X$	4) $TF_X^* \xrightarrow{\sigma_X'} TF_X + L_X$
5) $TF_Y + L_Y \xrightarrow{\sigma_Y} TF_Y^*$	5) $TF_Y + L_Y \xrightarrow{\sigma_Y} TF_Y^*$	5) $TF_Y + L_Y \xrightarrow{\sigma_Y} TF_Y^*$	5) $TF_Y + L_Y \xrightarrow{\sigma_Y} TF_Y^*$
6) $TF_Y^* \xrightarrow{\sigma_Y'} TF_Y + L_Y$	6) $TF_Y^* \xrightarrow{\sigma_Y'} TF_Y + L_Y$	6) $TF_Y^* \xrightarrow{\sigma_Y'} TF_Y + L_Y$	6) $TF_Y^* \xrightarrow{\sigma_Y'} TF_Y + L_Y$
7) $G_X + TF_Y^* \xrightarrow{\sigma_{PX}} G_X^*$	7) $G_X + TF_Y^* \xrightarrow{\sigma_{PX}} G_X^*$	7) $G_X + TF_Y^* \xrightarrow{\kappa_X} G_X^\ominus$	7) $G_X + TF_Y^* \xrightarrow{\kappa_X} G_X^\ominus$
8) $G_X^* \xrightarrow{\sigma_{PX'}} G_X + TF_Y^*$	8) $G_X^* \xrightarrow{\sigma_{PX'}} G_X + TF_Y^*$	8) $G_X^\ominus \xrightarrow{\kappa_X'} G_X + TF_Y^*$	8) $G_X^\ominus \xrightarrow{\kappa_X'} G_X + TF_Y^*$
9) $G_Y + TF_X^* \xrightarrow{\sigma_{PY}} G_Y^*$	9) $G_Y + TF_X^* \xrightarrow{\kappa_Y} G_Y^\ominus$	9) $G_Y + TF_X^* \xrightarrow{\sigma_{PY}} G_Y^*$	9) $G_Y + TF_X^* \xrightarrow{\kappa_Y} G_Y^\ominus$
10) $G_Y^* \xrightarrow{\sigma_{PY'}} G_Y + TF_X^*$	10) $G_Y^\ominus \xrightarrow{\kappa_Y} G_Y + TF_X^*$	10) $G_Y^* \xrightarrow{\sigma_{PY'}} G_Y + TF_X^*$	10) $G_Y^\ominus \xrightarrow{\kappa_Y} G_Y + TF_X^*$
11) $G_X^* \xrightarrow{\rho_X'} G_X^* + TF_X$	11) $G_X^* \xrightarrow{\rho_X'} G_X^* + TF_X$	11) $G_Y^* \xrightarrow{\rho_Y'} G_Y^* + TF_Y$	11) $TF_X \xrightarrow{k_{dX}} \phi$
12) $G_Y^* \xrightarrow{\rho_Y'} G_Y^* + TF_Y$	12) $TF_X \xrightarrow{k_{dX}} \phi$	12) $TF_X \xrightarrow{k_{dX}} \phi$	12) $TF_Y \xrightarrow{k_{dY}} \phi$
13) $TF_X \xrightarrow{k_{dX}} \phi$	13) $TF_Y \xrightarrow{k_{dY}} \phi$	13) $TF_Y \xrightarrow{k_{dY}} \phi$	
14) $TF_Y \xrightarrow{k_{dY}} \phi$			

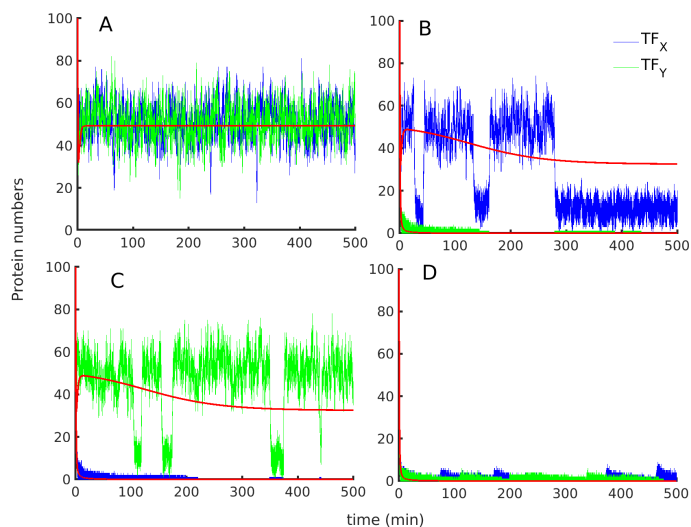


FIG. S2: Trajectories obtained for various FBL GRN motifs are presented here. Panel A, B, C, and D represent the positive feedback loop, the negative feedback loop of type I and II, and the mutually inhibiting feedback loop, respectively. The parameters associated with these results are given in the table S7.

C. FFL

TABLE S4: This table contains the reactions for the Coherent FFL network motif. Here, G_X, G_Y and G_A represent the genes with the basal expression, G_Y^* and G_A^* represent the activated genes, and G_Y^\ominus and G_A^\ominus represent the repressed genes. Also, TF_X, TF_Y and TF_A represent the proteins that are expressed by G_X, G_Y and G_A respectively. The specific reaction rates for each reaction are shown on the marked arrows.

Coherent T1	Coherent T2	Coherent T3	Coherent T4
1) $G_X \xrightarrow{\rho_X} G_X + TF_X$	1) $G_X \xrightarrow{\rho_X} G_X + TF_X$	1) $G_X \xrightarrow{\rho_X} G_X + TF_X$	1) $G_X \xrightarrow{\rho_X} G_X + TF_X$
2) $G_Y \xrightarrow{\rho_Y} G_Y + TF_Y$	2) $G_Y \xrightarrow{\rho_Y} G_Y + TF_Y$	2) $G_Y \xrightarrow{\rho_Y} G_Y + TF_Y$	2) $G_Y \xrightarrow{\rho_Y} G_Y + TF_Y$
3) $G_A \xrightarrow{\rho_A} G_A + TF_A$	3) $G_A \xrightarrow{\rho_A} G_A + TF_A$	3) $G_A \xrightarrow{\rho_A} G_A + TF_A$	3) $G_A \xrightarrow{\rho_A} G_A + TF_A$
4) $TF_X + L_X \xrightarrow{\sigma_X} TF_X^*$	4) $TF_X + L_X \xrightarrow{\sigma_X} TF_X^*$	4) $TF_X + L_X \xrightarrow{\sigma_X} TF_X^*$	4) $TF_X + L_X \xrightarrow{\sigma_X} TF_X^*$
5) $TF_X^* \xrightarrow{\sigma_X'} TF_X + L_X$	5) $TF_X^* \xrightarrow{\sigma_X'} TF_X + L_X$	5) $TF_X^* \xrightarrow{\sigma_X'} TF_X + L_X$	5) $TF_X^* \xrightarrow{\sigma_X'} TF_X + L_X$
6) $TF_Y + L_Y \xrightarrow{\sigma_Y} TF_Y^*$	6) $TF_Y + L_Y \xrightarrow{\sigma_Y} TF_Y^*$	6) $TF_Y + L_Y \xrightarrow{\sigma_Y} TF_Y^*$	6) $TF_Y + L_Y \xrightarrow{\sigma_Y} TF_Y^*$
7) $TF_Y^* \xrightarrow{\sigma_Y'} TF_Y + L_Y$	7) $TF_Y^* \xrightarrow{\sigma_Y'} TF_Y + L_Y$	7) $TF_Y^* \xrightarrow{\sigma_Y'} TF_Y + L_Y$	7) $TF_Y^* \xrightarrow{\sigma_Y'} TF_Y + L_Y$
8) $G_Y + TF_X^* \xrightarrow{\sigma_{PY}} G_Y^*$	8) $G_Y + TF_X^* \xrightarrow{\kappa_Y} G_Y^\ominus$	8) $G_Y + TF_X^* \xrightarrow{\sigma_{PY}} G_Y^*$	8) $G_Y + TF_X^* \xrightarrow{\kappa_Y} G_Y^\ominus$
9) $G_Y^* \xrightarrow{\sigma_{PY'}} G_Y + TF_X^*$	9) $G_Y^\ominus \xrightarrow{\kappa_Y'} G_Y + TF_X^*$	9) $G_Y^* \xrightarrow{\sigma_{PY'}} G_Y + TF_X^*$	9) $G_Y^\ominus \xrightarrow{\kappa_Y'} G_Y + TF_X^*$
10) $G_A + TF_X^* \xrightarrow{\sigma_{PA1'}} G_A^*$	10) $G_A + TF_X^* \xrightarrow{\kappa_A} G_A^\ominus$	10) $G_A + TF_X^* \xrightarrow{\kappa_A} G_A^\ominus$	10) $G_A + TF_X^* \xrightarrow{\sigma_{PA1'}} G_A^*$
11) $G_A^* \xrightarrow{\sigma_{PA1''}} G_A + TF_X^*$	11) $G_A^\ominus \xrightarrow{\kappa_A'} G_A + TF_X^*$	11) $G_A^\ominus \xrightarrow{\kappa_A'} G_A + TF_X^*$	11) $G_A^* \xrightarrow{\sigma_{PA1''}} G_A + TF_X^*$
12) $G_A + TF_Y^* \xrightarrow{\sigma_{PA2}} G_A^{**}$	12) $G_A + TF_Y^* \xrightarrow{\sigma_{PA2'}} G_A^*$	12) $G_A^\ominus + TF_Y^* \xrightarrow{\kappa_{A2}} G_A^\ominus$	12) $G_A + TF_Y^* \xrightarrow{\kappa_A} G_A^\ominus$
13) $G_A^{**} \xrightarrow{\sigma_{PA2''}} G_A^* + TF_Y^*$	13) $G_A^* \xrightarrow{\sigma_{PA2''}} G_A + TF_Y^*$	13) $G_A^{\ominus\ominus} \xrightarrow{\kappa_{AA'}} G_A^\ominus + TF_Y^*$	13) $G_A^\ominus \xrightarrow{\kappa_A'} G_A + TF_Y^*$
14) $G_Y^* \xrightarrow{\rho_{Y'}} G_Y^* + TF_Y$	14) $G_A^* \xrightarrow{\rho_A'} G_A^* + TF_A$	14) $G_Y^* \xrightarrow{\rho_{Y'}} G_Y^* + TF_Y$	14) $G_A^* \xrightarrow{\rho_A'} G_A^* + TF_A$
15) $G_A^* \xrightarrow{\rho_{PA'}} G_A^* + TF_A$	15) $TF_X \xrightarrow{k_{dX}} \phi$	15) $TF_X \xrightarrow{k_{dX}} \phi$	15) $TF_X \xrightarrow{k_{dX}} \phi$
16) $G_A^{**} \xrightarrow{\rho_{PA''}} G_A^{**} + TF_A$	16) $TF_Y \xrightarrow{k_{dY}} \phi$	16) $TF_Y \xrightarrow{k_{dY}} \phi$	16) $TF_Y \xrightarrow{k_{dY}} \phi$
17) $TF_X \xrightarrow{k_{dA}} \phi$	17) $TF_A \xrightarrow{k_{dA}} \phi$	17) $TF_A \xrightarrow{k_{dA}} \phi$	17) $TF_A \xrightarrow{k_{dA}} \phi$
18) $TF_Y \xrightarrow{k_{dY}} \phi$			
19) $TF_A \xrightarrow{k_{dA}} \phi$			

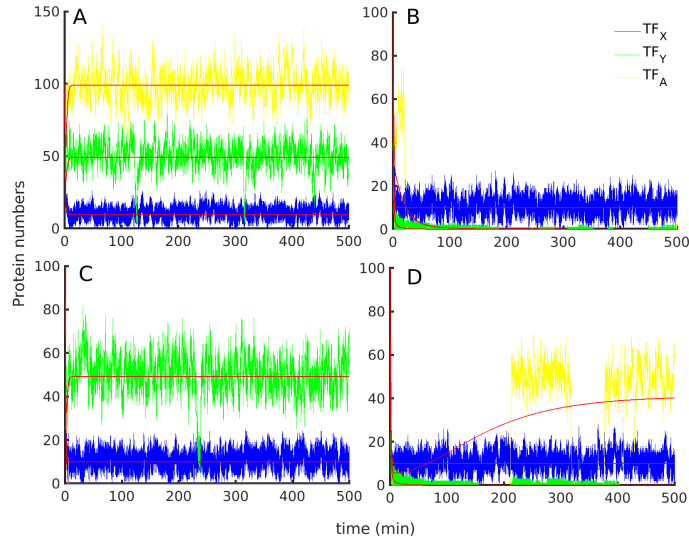


FIG. S3: Trajectories for the coherent FFL GRN motifs. Here panel A,B,C and D refer to the coherent FFL type 1,2,3 and 4 respectively. The parameters associated with these results are given in the table S7.

TABLE S5: This table contains the reactions for the incoherent FFL network motif. Here, G_X, G_Y and G_A represent the genes with the basal expression, G_Y^* and G_A^* represent the activated genes, and G_Y^\ominus and G_A^\ominus represent the repressed genes. Also, TF_X, TF_Y and TF_A represent the proteins that are expressed by G_X, G_Y and G_A respectively.

Incoherent T1	Incoherent T2	Incoherent T3	Incoherent T4
1) $G_X \xrightarrow{\rho_X} G_X + TF_X$	1) $G_X \xrightarrow{\rho_X} G_X + TF_X$	1) $G_X \xrightarrow{\rho_X} G_X + TF_X$	1) $G_X \xrightarrow{\rho_X} G_X + TF_X$
2) $G_Y \xrightarrow{\rho_Y} G_Y + TF_Y$	2) $G_Y \xrightarrow{\rho_Y} G_Y + TF_Y$	2) $G_Y \xrightarrow{\rho_Y} G_Y + TF_Y$	2) $G_Y \xrightarrow{\rho_Y} G_Y + TF_Y$
3) $G_A \xrightarrow{\rho_A} G_A + TF_A$	3) $G_A \xrightarrow{\rho_A} G_A + TF_A$	3) $G_A \xrightarrow{\rho_A} G_A + TF_A$	3) $G_A \xrightarrow{\rho_A} G_A + TF_A$
4) $TF_X + L_X \xrightarrow{\sigma_X} TF_X^*$	4) $TF_X + L_X \xrightarrow{\sigma_X} TF_X^*$	4) $TF_X + L_X \xrightarrow{\sigma_X} TF_X^*$	4) $TF_X + L_X \xrightarrow{\sigma_X} TF_X^*$
5) $TF_X^* \xrightarrow{\sigma_X'} TF_X + L_X$	5) $TF_X^* \xrightarrow{\sigma_X'} TF_X + L_X$	5) $TF_X^* \xrightarrow{\sigma_X'} TF_X + L_X$	5) $TF_X^* \xrightarrow{\sigma_X'} TF_X + L_X$
6) $TF_Y + L_Y \xrightarrow{\sigma_Y} TF_Y^*$	6) $TF_Y + L_Y \xrightarrow{\sigma_Y} TF_Y^*$	6) $TF_Y + L_Y \xrightarrow{\sigma_Y} TF_Y^*$	6) $TF_Y + L_Y \xrightarrow{\sigma_Y} TF_Y^*$
7) $TF_Y^* \xrightarrow{\sigma_Y'} TF_Y + L_Y$	7) $TF_Y^* \xrightarrow{\sigma_Y'} TF_Y + L_Y$	7) $TF_Y^* \xrightarrow{\sigma_Y'} TF_Y + L_Y$	7) $TF_Y^* \xrightarrow{\sigma_Y'} TF_Y + L_Y$
8) $G_Y + TF_X^* \xrightarrow{\sigma_{PY}} G_Y^*$	8) $G_Y + TF_X^* \xrightarrow{\kappa_Y} G_Y^\ominus$	8) $G_Y + TF_X^* \xrightarrow{\sigma_{PY}} G_Y^*$	8) $G_Y + TF_X^* \xrightarrow{\kappa_Y} G_Y^\ominus$
9) $G_Y^* \xrightarrow{\sigma_{PY'}} G_Y + TF_X^*$	9) $G_Y^\ominus \xrightarrow{\kappa_Y'} G_Y + TF_X^*$	9) $G_Y^* \xrightarrow{\sigma_{PY'}} G_Y + TF_X^*$	9) $G_Y^\ominus \xrightarrow{\kappa_Y'} G_Y + TF_X^*$
10) $G_A + TF_X^* \xrightarrow{\sigma_{PA1'}} G_A^*$	10) $G_A + TF_X^* \xrightarrow{\kappa_{A1}} G_A^\ominus$	10) $G_A + TF_X^* \xrightarrow{\kappa_A} G_A^\ominus$	10) $G_A + TF_X^* \xrightarrow{\sigma_{PA1'}} G_A^*$
11) $G_A^* \xrightarrow{\sigma_{PA1'}} G_A + TF_X^*$	11) $G_A^\ominus \xrightarrow{\kappa_{A1}'} G_A + TF_X^*$	11) $G_A^\ominus \xrightarrow{\kappa_{A1}'} G_A + TF_X^*$	11) $G_A^* \xrightarrow{\sigma_{PA1'}} G_A + TF_X^*$
12) $G_A + TF_Y^* \xrightarrow{\kappa_A} G_A^\ominus$	12) $G_A^\ominus + TF_Y^* \rightarrow$	12) $G_A + TF_Y^* \xrightarrow{\sigma_{PA1'}} G_A^*$	12) $G_A^* + TF_Y^* \xrightarrow{\sigma_{PA2'}} G_A^{**}$
13) $G_A^\ominus \xrightarrow{\kappa_{A1}'} G_A + TF_Y^*$	13) $G_A^{\ominus\ominus} \xrightarrow{\kappa_{A2}} G_A^\ominus + TF_Y^*$	13) $G_A^* \xrightarrow{\sigma_{PA1'}} G_A + TF_Y^*$	13) $G_A^{**} \xrightarrow{\sigma_{PA1'}} G_A^* + TF_Y^*$
14) $G_Y^* \xrightarrow{\rho_{Y'}} G_Y^* + TF_Y$	14) $TF_X \xrightarrow{k_{dX}} \phi$	14) $G_Y^* \xrightarrow{\rho_{Y'}} G_Y^* + TF_Y$	14) $G_A^* \xrightarrow{\rho_{A1}'} G_A^* + TF_A$
15) $G_A^* \xrightarrow{\rho_{PA'}} G_A^* + TF_A$	15) $TF_Y \xrightarrow{k_{dY}} \phi$	15) $G_A^* \xrightarrow{\rho_{PA'}} G_A^* + TF_A$	15) $G_A^{**} \xrightarrow{\rho_{PA''}} G_A^* + TF_A$
16) $TF_X \xrightarrow{k_{dX}} \phi$	16) $TF_A \xrightarrow{k_{dA}} \phi$	17) $TF_X \xrightarrow{k_{dX}} \phi$	17) $TF_X \xrightarrow{k_{dX}} \phi$
17) $TF_Y \xrightarrow{k_{dY}} \phi$		17) $TF_Y \xrightarrow{k_{dY}} \phi$	17) $TF_Y \xrightarrow{k_{dY}} \phi$
18) $TF_A \xrightarrow{k_{dA}} \phi$		18) $TF_A \xrightarrow{k_{dA}} \phi$	18) $TF_A \xrightarrow{k_{dA}} \phi$

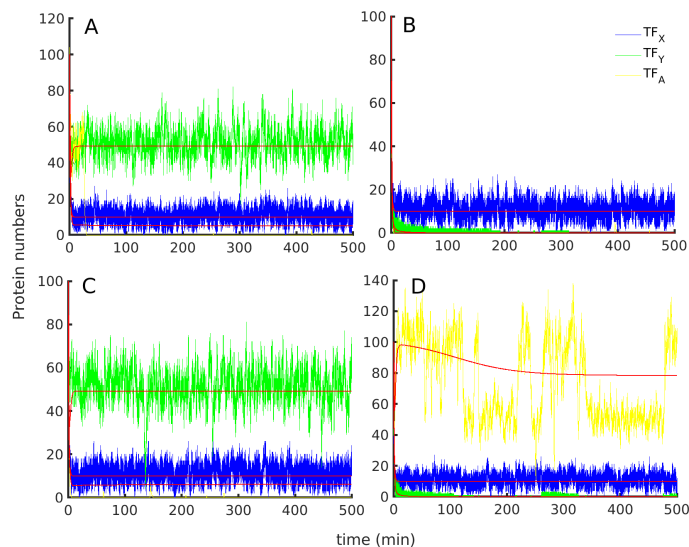


FIG. S4: Trajectories for the incoherent FFL GRN motifs. Here panel A,B,C and D refer to the incoherent FFL type 1,2,3 and 4 respectively. Here red colored line for all the cases corresponds to the deterministic results. The parameters associated with these results are given in the table S7.

III. KINETIC MONTE CARLO SIMULATION

Kinetic Monte Carlo (KMC), also known as dynamic Monte Carlo, is a numerical tool used to calculate the system's stochastic evolution. KMC dispenses individual realizations of the Markov process defined by a few elementary reactions. It has numerous applicability in many systems, i.e., biology, ecology, chemical reaction dynamics, etc. Here, We employed the Gillespie algorithm to perform the KMC simulation for the various gene regulatory network motifs. The change in states for the various vector species $[G_i G_i^* G_i^{**} G_i^\ominus G_i^{\ominus\ominus} TF_i TF_i^* L_i]$ where $i \in (X, Y, A)$ are presented in the tables. Also, a_0 represents the propensity function. Thus, we have performed KMC and updated the corresponding protein production and degradation for these elementary events with their corresponding rate constants. The algorithm is straightforward, considers intrinsic noises, and operates in continuous time space and discrete reaction space. According to the algorithm, it first calculates the propensity function followed by drawing two random numbers (r1 and r2) from a uniform distribution in the interval (0, 1). The use of the first random number, r1, is to stochastic update of time ($t+\tau$) during the occurrence of the next reaction, where $\tau = \frac{1}{a_0} \ln \frac{1}{r_1}$, where $a_0 = \sum_{i=1}^n a_i$, and n in the occurring event. A reaction is chosen randomly based on the criteria, $\sum_{i=1}^{n-1} a_i < r_2 a_0 \leq \sum_{i=1}^n a_i$. The system states updated after τ interval according to the stoichiometric matrix, S of the reacting system as $X(t+\tau) = X(t)+S$.

IV. PARAMETERS

TABLE S6: Parameters used for the various network motifs in the main text are presented here. The symbols $\epsilon_{X,Y}$, ϵ_{R_X,R_Y,R_A} are the binding interaction energy parameters for TF, RNAP and operator interaction. ϵ_{LP} is the bending energy for the formation DNA loops between operators.

Network Motifs	Type	Symbols	Values/ $k_B T$	References
Simple Activation/Repression		$\epsilon_{R_X}=\epsilon_{R_Y}$	-2.9	[2-4]
		ϵ_Y	-10	[3]
		$\epsilon_{R_Y Y}$	-3	[4]
		ϵ_{nn}	-1	[2]
		$\lambda_{R_X}=\lambda_{R_Y}$	$10^{-4}/k_B T$	[2]
		λ_Y	$1.5 \times 10^{-6}/k_B T$	[5]
Feedback Loops		$\epsilon_{R_X}=\epsilon_{R_Y}$	-2.9	[2-4]
		$\epsilon_X=\epsilon_Y$	-10	[3]
	PFL	$\epsilon_{R_X X}=\epsilon_{R_Y Y}$	-3	[2, 4, 5]
	NFL1	$\epsilon_{R_X X}$	-3	
	NFL1	$\epsilon_{R_Y Y}$	3	
	NFL2	$\epsilon_{R_X X}$	3	
	NFL2	$\epsilon_{R_Y Y}$	-3	
	FNFL	$\epsilon_{R_X X}=\epsilon_{R_Y Y}$	3	
		$\lambda_{R_X}=\lambda_{R_Y}$	$10^{-4}/k_B T$	[2]
		$\lambda_X=\lambda_Y$	$1.5 \times 10^{-6}/k_B T$	[5]
Feedforward Loops		$\epsilon_{R_X}=\epsilon_{R_Y}=\epsilon_{R_A}$	-2.9	[2-4]
		$\epsilon_X=\epsilon_Y=\epsilon_A$	-10	[3]
		ϵ_{LP}	10	[3]
		$\epsilon_{s_Y}=\epsilon_{s_A}^A=\epsilon_{s_A}$	-3	[2, 4, 5]
		ϵ_{nn}	-1	[2]
	Coherent T1	$\epsilon_{R_Y Y}=\epsilon_{R_A Y}^A=\epsilon_{R_A Y}$	-3	[2, 4, 5]
	Coherent T2	$\epsilon_{R_A Y}$	-3	
	Coherent T2	$\epsilon_{R_Y Y}=\epsilon_{R_A Y}^A$	0	
	Coherent T3	$\epsilon_{R_Y Y}$	-3	
	Coherent T3	$\epsilon_{R_A Y}^A=\epsilon_{R_A Y}$	0	
	Coherent T4	$\epsilon_{R_A Y}^A$	-3	
	Coherent T4	$\epsilon_{R_Y Y}=\epsilon_{R_A Y}$	0	
	Incoherent T1	$\epsilon_{R_Y Y}=\epsilon_{R_A Y}^A$	-3	
	Incoherent T1	$\epsilon_{R_A Y}$	0	
	Incoherent T2	$\epsilon_{R_Y Y}=\epsilon_{R_A Y}^A=\epsilon_{R_A Y}$	0	
	Incoherent T3	$\epsilon_{R_Y Y}=\epsilon_{R_A Y}$	-3	
	Incoherent T3	$\epsilon_{R_A Y}^A$	0	
	Incoherent T4	$\epsilon_{R_A Y}^A=\epsilon_{R_A Y}$	-3	
	Incoherent T4	$\epsilon_{R_Y Y}$	0	
		$\lambda_{R_X}=\lambda_{R_Y}=\lambda_{R_A}$	$10^{-4}/k_B T$	[2, 3]
		$\lambda_X=\lambda_Y=\lambda_A$	$1.5 \times 10^{-6}/k_B T$	[5]

TABLE S7: Different values of parameters used in our kinetic calculations are presented here. Symbols ρ_X , ρ_Y , and ρ_A are the forward rate constants for the production of corresponding TF and the prime values of the same are the rate constants associated with the stimulated forms. Similarly, σ_X , σ_Y and their prime values indicate the forward and backward rate constants for the formation of stimulated TF's respectively. Also, σ_{P_X} , σ_{P_Y} and their prime values indicate the forward and backward rate constants for the formation of activated promoters respectively. Similarly, κ_X , κ_Y and κ_A and their prime values indicate the forward and backward rate constants for the formation of repressed promoters respectively.

Parameters	Values	References
$\rho_X = \rho_Y = \rho_A$	10 min^{-1}	[6]
$\sigma_X = \sigma_Y$	$60 \text{ mol}^{-1}\text{min}^{-1}$	[7]
$\kappa_X = \kappa_Y = \kappa_A$	0.1 min^{-1}	
$\sigma'_X = \sigma'_Y$	60 min^{-1}	[6, 8]
$\kappa'_X = \kappa'_Y = \kappa'_A$	0.01 min^{-1}	
$\sigma_{P_X} = \sigma_{P_Y}$	$0.0126 \text{ mol}^{-1}\text{min}^{-1}$	[6, 7]
$\sigma'_{P_X} = \sigma'_{P_Y}$	$0.01 \text{ mol}^{-1}\text{min}^{-1}$	[6]
$\rho'_X = \rho'_Y = \rho'_A$	50 min^{-1}	[7]
ρ_A	100 min^{-1}	
k_{dX}	1 min^{-1}	[6, 8]
k_{dY}	1 min^{-1}	[6, 7]

TABLE S8: Parameters used for thermodynamic modeling of the gene regulation of *Gal* promoter in a yeast cell are presented in the table.

Parameters	Symbols	Values	References
Mig1, Tup1 and glucose	$\epsilon_{Mig1p-Tup1p}$	$-17.4k_B T$	[3]
	$\epsilon_{Mig1p-DNA}$	$-20.72k_B T$	
	λ_{Mig1p}	10^{-6}	[3]
	λ_{Tup1p}	2.5×10^{-6}	[3]
Gal4, Gal80 and galactose	$\epsilon_{Gal80p-Gal3p}$	$-18.5k_B T$	[5]
	$\epsilon_{Gal4p-DNA}$	$-20k_B T$	[5]
	$w_{Gal4p-RNAP}$	$-3k_B T$	[5]
	λ_{Gal80p}	4×10^{-7}	[3]
	λ_{Gal4p}	10^{-6}	[3]
RNAP	$q_R \lambda_R$	0.298	[5]

TABLE S9: Parameters used for the kinetic modeling of gene regulation of *Gal* promoter in a yeast cell are presented in the table.

Parameters	Values	References
$\rho_1 = \rho_2 = \rho_3$	10 min^{-1}	[9, 10]
$\sigma_a = \sigma_b$	$60 \text{ mol}^{-1}\text{min}^{-1}$	[9]
$\kappa_{PA} = \kappa_{PB}$	$0.01 \text{ mol}^{-1}\text{min}^{-1}$	[10]
$\sigma_{PA} = \sigma_{PB} = \sigma_{PC}$	$0.0126 \text{ mol}^{-1}\text{min}^{-1}$	[9, 11]
$\rho'_1 = \rho'_2 = \rho'_3$	100 min^{-1}	[9, 10]
$\sigma'_a = \sigma'_b$	60 min^{-1}	[9, 12]
$\kappa'_{PA} = \kappa'_{PB}$	0.0126 min^{-1}	[9, 12]
$\sigma'_{PA} = \sigma'_{PB} = \sigma'_{PC}$	0.01 min^{-1}	[11]

V. COMPLEX ASSEMBLIES FOR VARIOUS FBL GRN MOTIFS.

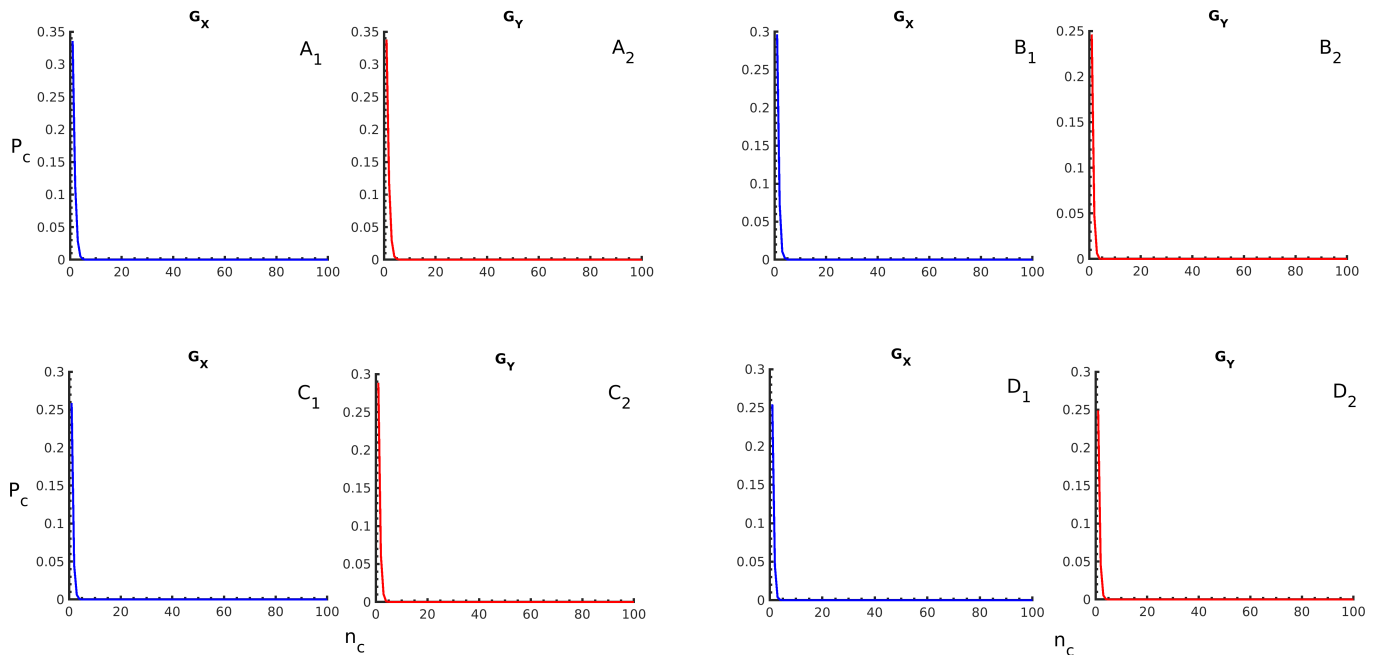


FIG. S5: Probability distributions of TAC on G_X and G_Y for the FL network are presented. Here A_1, A_2 represent PFL, B_1, B_2 represent NFL1, C_1, C_2 represent NFL2 and D_1, D_2 represent FNFL. The calculations are done at a fixed activity of TF molecules, $\lambda_{TF} = 10^1$. The parameters associated with these results are given in the table S6.

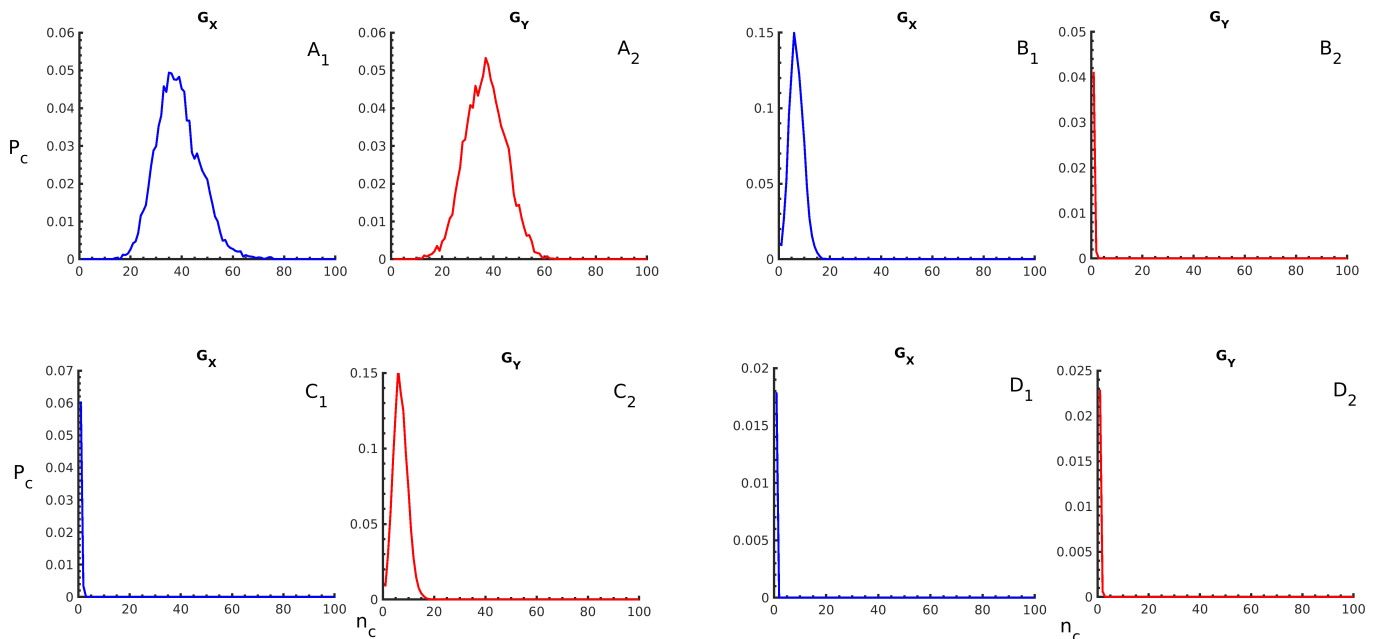


FIG. S6: Probability distributions of TAC on G_X and G_Y for the FL network are presented. Here A_1, A_2 represent PFL, B_1, B_2 represent NFL1, C_1, C_2 represent NFL2 and D_1, D_2 represent FNFL. The calculations are done at a fixed activity of TF molecules, $\lambda_{TF} = 10^3$. The parameters associated with these results are given in the table S6.

In figure S5, S6 and S7 we have calculated the distribution function of the complexes for three values of λ_{TF} i.e., 10^1 , 10^3 , 10^5 for G_X and G_Y . The detailed discussion is presented in the main text.

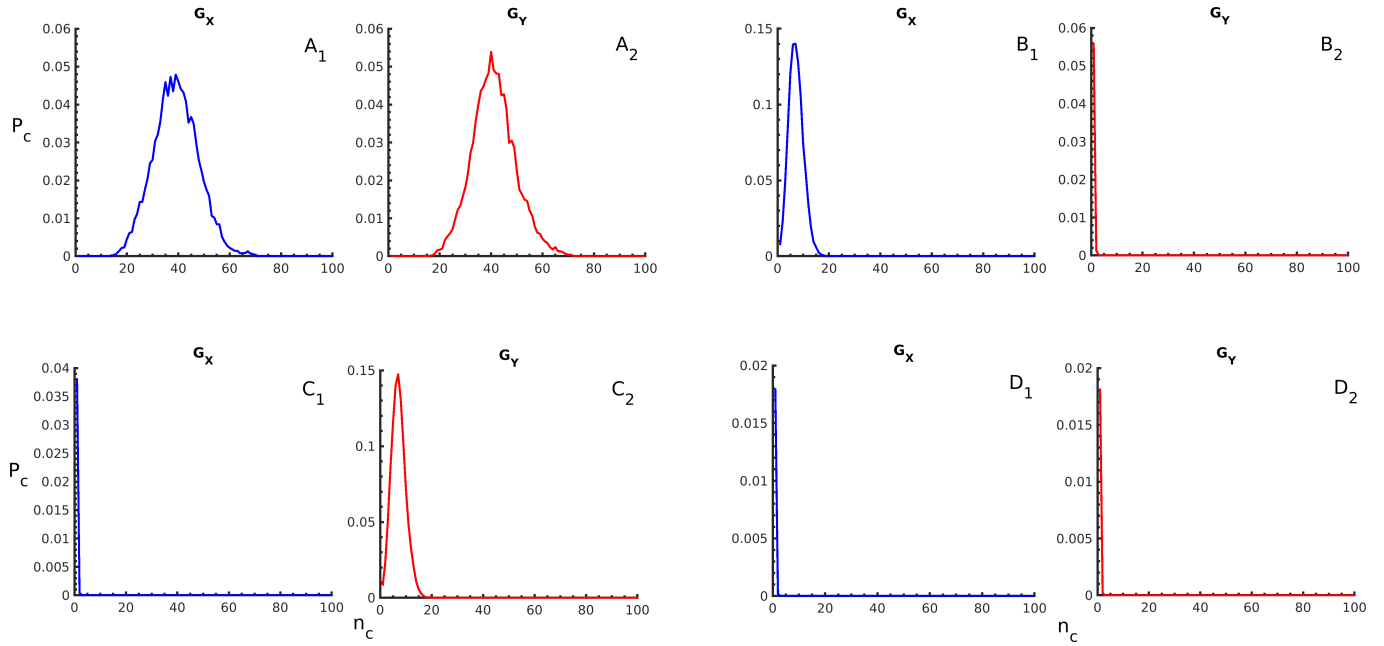


FIG. S7: Probability distributions of TAC on G_X and G_Y for the FL network are presented. Here A_1, A_2 represent PFL, B_1, B_2 represent NFL1, C_1, C_2 represent NFL2 and D_1, D_2 represent FNFL. The calculations are done at a fixed activity of TF molecules, $\lambda_{TF} = 10^5$. The parameters associated with these results are given in the table S6.

VI. GRAND CANONICAL PARTITION FUNCTION BASED CALCULATIONS FOR FFL NETWORKS

A. Coherent FFL

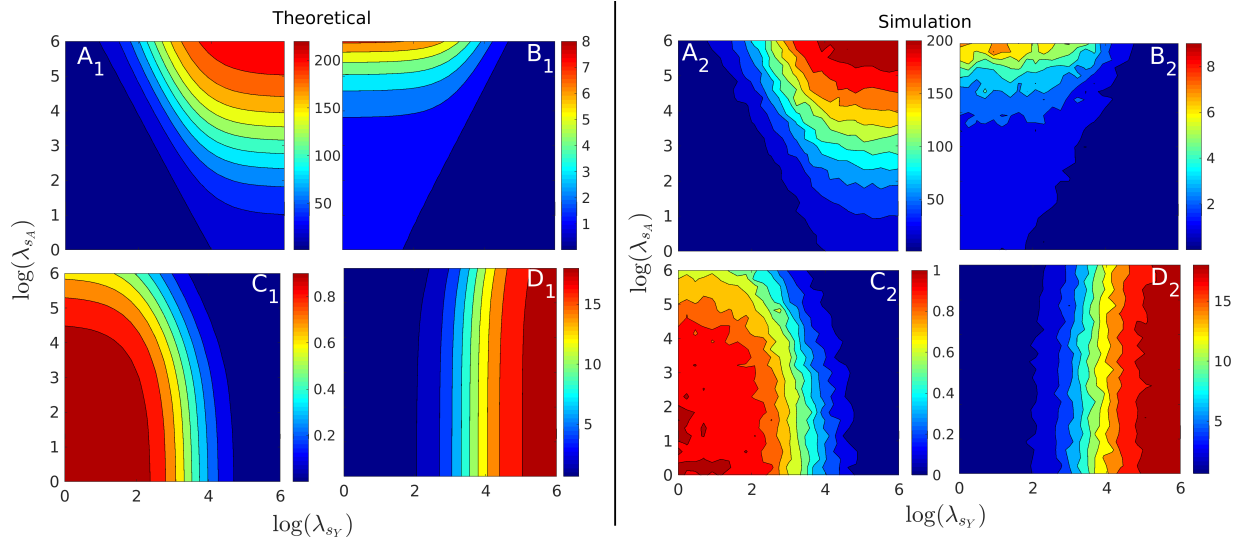


FIG. S8: Results obtained from the grand canonical partition function and MC simulations for the coherent FFL networks are presented. We consider only the specific interactions based on the network topology in these calculations. However, we ignore the long-range (interactions through DNA looping) and short-range (nearest neighbor) interactions to avoid mathematical complexity. Here, A1, B1, C1, and D1 represent coherent FFL of types 1,2,3, and 4 for the theoretical calculations in the non-interacting regime. The parameters associated with these results are given in the table S6.

B. Incoherent FFL

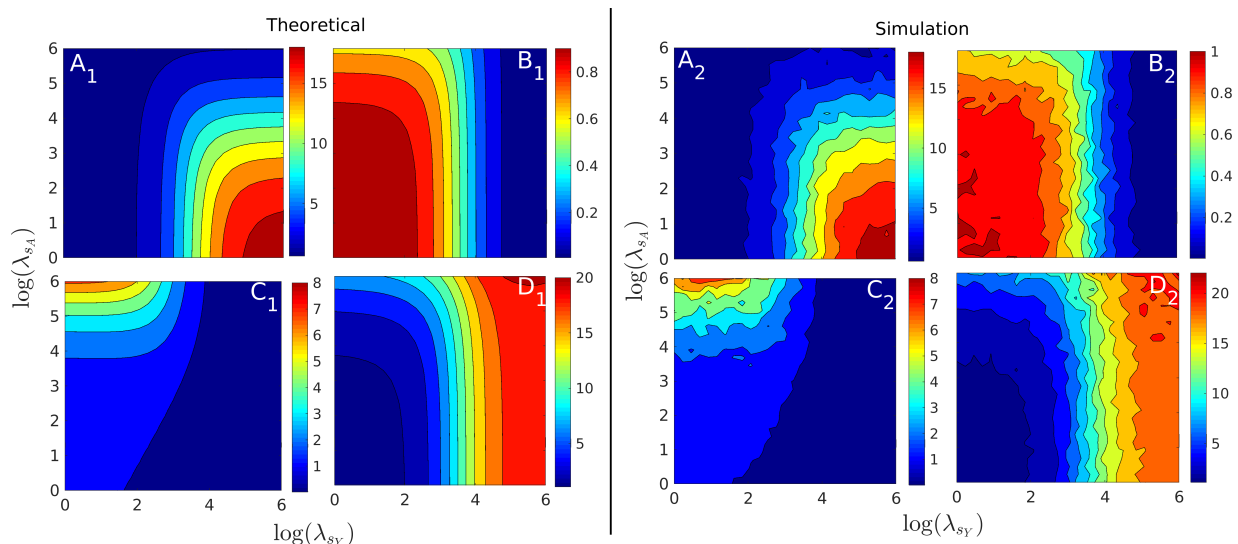


FIG. S9: Results obtained from the grand canonical partition function and MC simulations of incoherent FFL networks are presented here. We consider only the specific interactions based on the network topology in these calculations. However, we ignore the long-range (interactions through DNA looping) and short-range (nearest neighbor) interactions to avoid mathematical complexity. Here, A2, B2, C2, and D2 represent incoherent FFL of types 1,2,3, and 4 for the simulation results in the non-interacting regime. The parameters associated with these results are given in the table S6.

We have observed a good correlation between the theoretical and GCMC simulations as obtained for various FFL's network motifs(as presented in the main text) and the corresponding response curves presented in the figures S8 and S9 from theoretical calculations.

VII. ENTROPY CALCULATIONS FOR THE COMPLEX ASSEMBLIES FOR THE ACTIVATION AND REPRESSION OF GRN MOTIFS ARE PRESENTED. THE CALCULATIONS ARE ALSO DONE IN THE PRESENCE/ABSENCE OF SIGNALING SPECIES.

Here we have calculated Gibbs entropy (S) for various GRN motifs to estimate the reliability of the response functions. S has a functional form, $S = -R \sum_i o_i \log_e o_i$ where the variable o_i is the probability or the fraction of complex i on the promoter regions of the genes in a configuration.

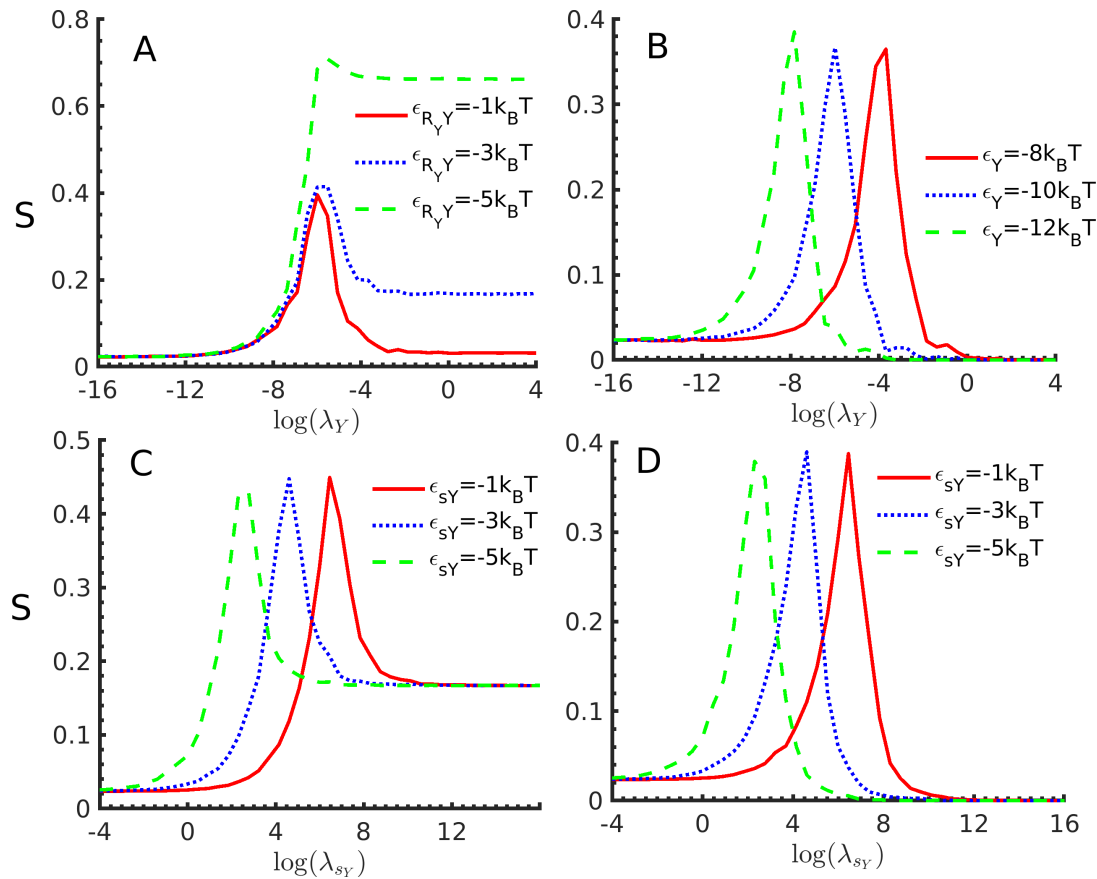


FIG. S10: Entropy(S) for the complexes as obtained for the activation and repression GRNs motif are presented. Here panel A,B,C and D refer to simple activation, repression, induced activation and repression respectively. The parameters associated with these results are given in the table S6.

It is observed in figure S10 that the higher value of S is associated with the co-existence of multiple bio-molecular species for the respective network motifs. Its detailed explanation is given in the main text.

VIII. ENTROPY CALCULATIONS FOR THE COMPLEX ASSEMBLIES FOR VARIOUS FBL GRN MOTIFS.

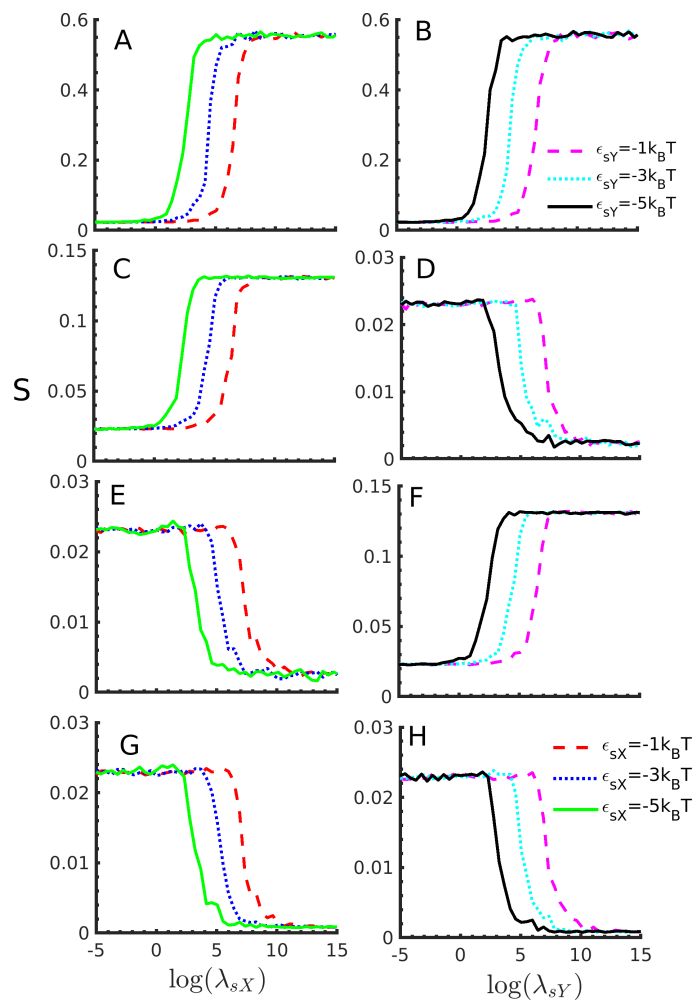


FIG. S11: The entropy of complexes obtained for various FBL GRN motifs is presented here. LHS panels correspond to G_X , and RHS panels correspond to G_Y . Panel (A, B),(C, D),(E, F), and (G, H) represent the positive feedback loop, the negative feedback loop of type I, II, and fully negative feedback loop, respectively. The parameters associated with these results are given in the table S6.

It can be seen in figure S11 that the S values give the same pattern as that of response function (given in the main text). Thus, FC and S shows a characteristic of entropy-driven signal transduction which is discussed in the main text in detail.

IX. ENTROPY CALCULATIONS FOR THE FFL

A. Entropy calculations for the coherent FFL

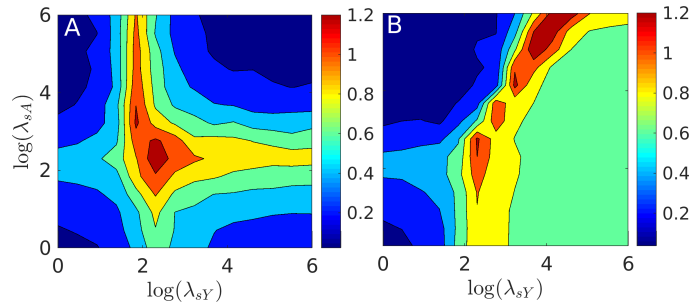


FIG. S12: Entropy of complexes obtained for coherent FFL GRN motifs. Here panel A and B refer to the coherent FFL type 3 and 4 respectively. The parameters associated with these results are given in the table S6.

B. Entropy calculations for the incoherent FFL

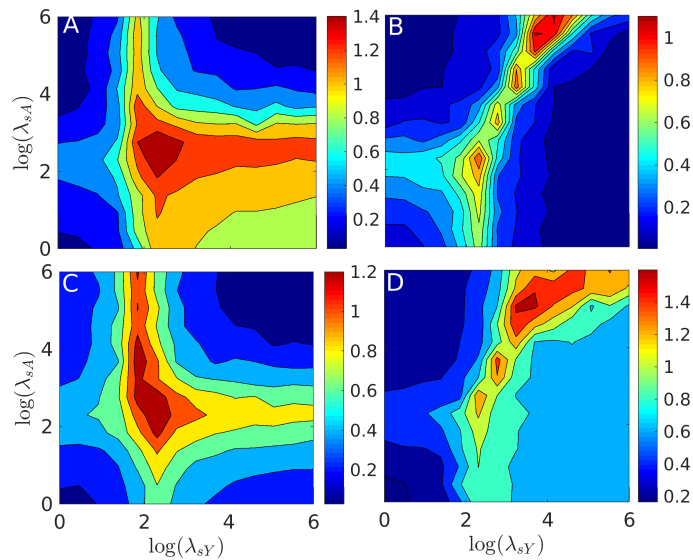


FIG. S13: Entropy of complexes obtained for incoherent FFL GRN motifs. Here panel A, B, C and D refer to the incoherent FFL type 1, 2, 3 and 4 respectively. The parameters associated with these results are given in the table S6.

In figures S12 and S13 we have observed that higher values of entropy is associated with the region where multiple complexes are coexisting at different values of λ_{sY} and λ_{sA} .

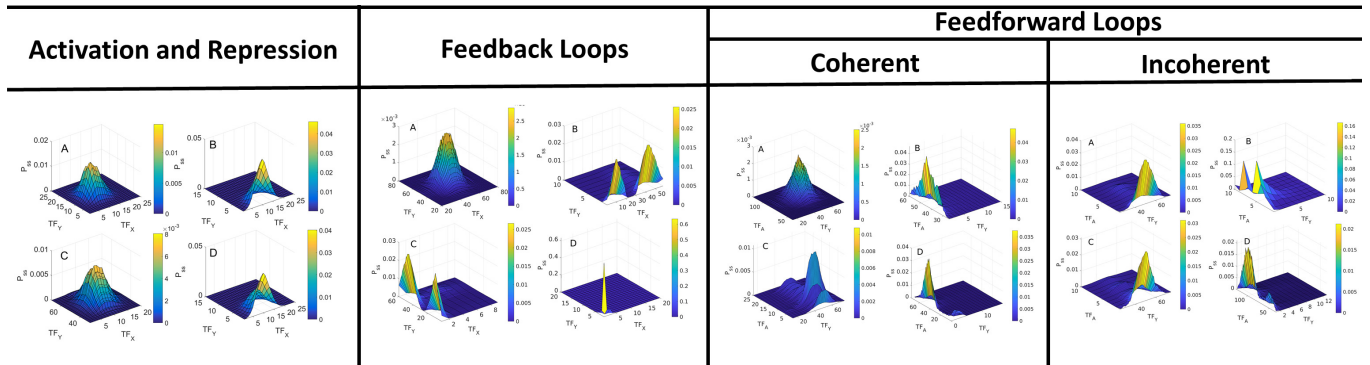


FIG. S14: The probability distribution of proteins obtained from stochastic simulation is shown here. The presented results are for the activation and repression, feedback loops, and feedforward loops. A clear signature of multimodality for higher-order network assembly is visible from this analysis. The parameters associated with these results are given in the table S8.

X. GAL GENES IN A YEAST CELL

A. Thermodynamic Model for a Gal promoter in a yeast cell

As discussed in the main text, galactose triggers the decision to express GAL genes, whereas glucose inhibits it. This complex assembly has two key TFs, i.e., Gal4p and Mig1p protein. Gal4p behaves as an activator for the expression of GAL genes, whereas Mig1p acts as a repressor. In the absence of galactose, Gal80p binds to Gal4p, which reduces its ability as an activator. Also, when glucose is present in abundance, it activates Mig1p by recruiting Tup1p, forming a heteromeric complex. Tup1p behaves as a histone deacetylase (HDAC), making the DNA less accessible for transcription. Thus, the expression of Gal genes is turned off in the presence of glucose. Galactose activates the expression of GAL genes by binding to Gal3p. The Gal80p has more affinity for Gal3p than Gal4p. Thus, galactose turns the expression of Gal genes ON. This whole assembly thus leads to the formation of dual feedback loops consisting of the positive and fully negative feedback loops.

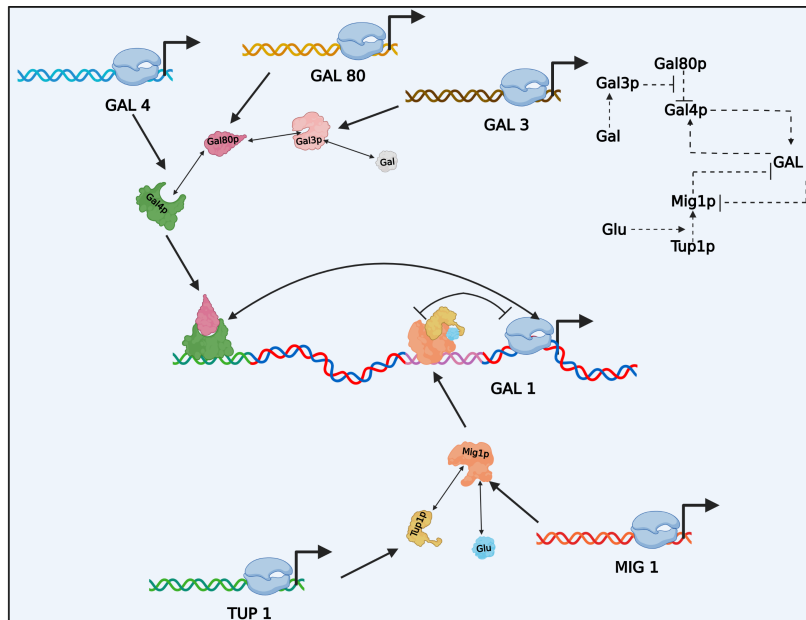


FIG. S15: Schematic figure showing the network of genetic assembly for Gal responsive genes in a yeast cell is presented.

The probability of occupation of galactose responsive gene or ON expression level as a function of glucose activity (λ_{glu}) for the wild-type, $mig1\Delta$, $gal80\Delta$, and $mig1\Delta$, $gal80\Delta$ strains is given by

$$P_{ON} = P_{max} \frac{1}{1+q_{glu}\lambda_{glu}} \quad (S6)$$

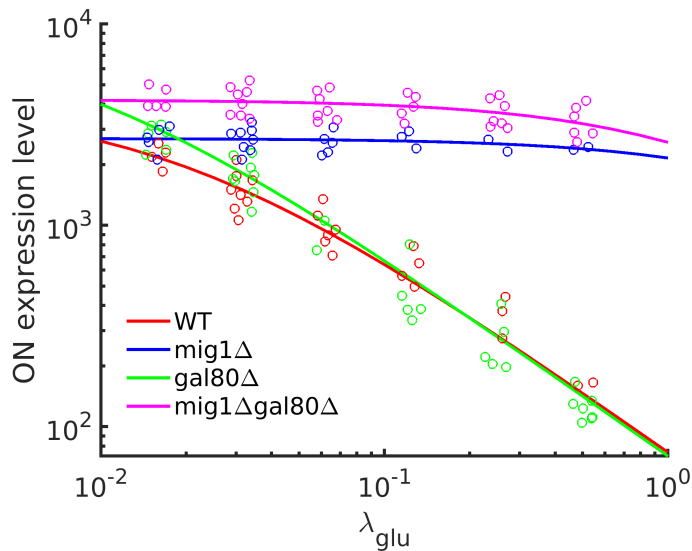


FIG. S16: On expression level of gal responsive genes is presented as a function of glucose activity. Solid lines indicate the experimental results and circles represent our simulated data. The expressions of various mutated variants are marked by different their legends.

On a final note, a correct understanding of the molecular mechanism behind complex computations of GRNs, equilibrium statistical mechanics, and its numerical version, such as MC simulations, is quite successful in predicting the gene expression. We show that only a few complex assemblies on DNA can do such a difficult task, which we have explored quantitatively using them. Estimating populations of such complexes is challenging from an *in vitro* experiment. Still, our modeling schemes allow one to connect experimental findings, as evident from our analysis. We show that the distribution function can be controlled externally by stabilizing or destabilizing complex assembly, which is crucial for developing a strategy for curing diseases.

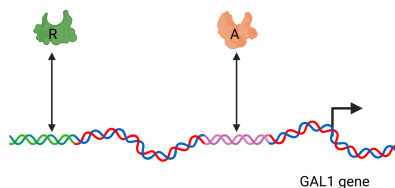


FIG. S17: Bio-molecular network for the activator and repressor binding on GAL1 gene.

We have observed a good correlation between the published data[13] and our simulation results in the figure S16. Expression of gal genes is observed to be decreasing for different strains as the concentration of glucose increases. The system, as mentioned above, creates a borderline for a yeast cell to use glucose and galactose as a source of energy when both of them are present in the environment in different quantities. This is known as ratio-sensing, as explained in the main text. Here, we consider a case where two biomolecules, an activator(A) and repressor(R), bind to the

promoter of a GAL1 gene. A signaling molecule controls the levels of these biomolecules. The fraction of bound sites by input molecule A is,

$$(S7) \quad P_{ON} = \frac{1}{1+q_A\lambda_A+q_R\lambda_R+q_A\lambda_Aq_R\lambda_R}$$

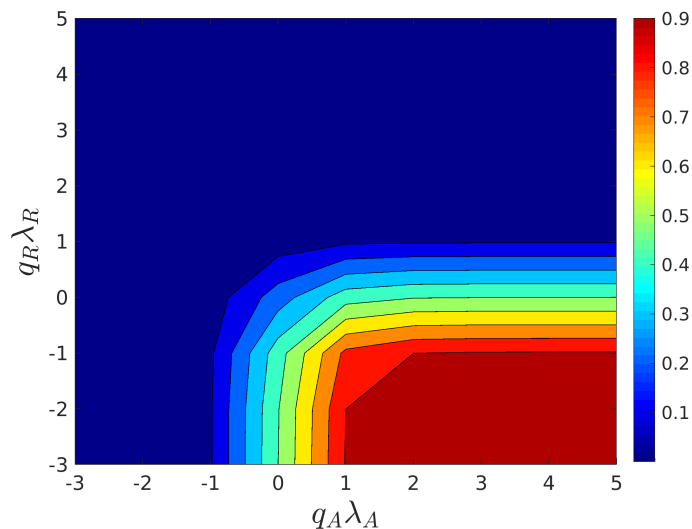


FIG. S18: Ratio output is presented for a simple module that consists of two input biomolecules i.e. activator(A) and repressor(R) where they bind to a promoter of GAL gene as shown in the figure S17.

In figure S18, ratio output is presented as a function of transcription activity of Gal4p or activator(A) and Mig1p or repressor(R). We have compared our simulation results with the published data[14] for this ratio-sensing and the excellent correlation we have observed in this figure. It was reported[14] that the ratio of galactose:glucose controls the expression of gal genes which is known as "ratio-sensing." As demonstrated here, we show that our modeling scheme perfectly works well for this GRN system. Let q_M, q_G and q_R represent the site partition functions for Mig1p, Gal4p and RNAP bio-molecules. Also, λ_M, λ_G , and λ_R represent the Mig1p, Gal4p, and RNAP bio-molecules activities, we can formulate the grand partition function and calculate the probabilities for the formation of complex assemblies.

$$(S8) \quad \begin{aligned} \xi_{ON} &= q_R\lambda_R + q_G\lambda_Gq_R\lambda_R e^{-\frac{w_{GR}}{k_B T}}; \\ \xi_{OFF} &= q_M\lambda_M + q_G\lambda_G \\ \xi &= 1 + \xi_{ON} + \xi_{OFF} \end{aligned}$$

Therefore, we can calculate the fraction of RNAP on the promoter (\bar{o}_P) for Gal1 gene as follows :

$\bar{o}_P = \frac{\xi_{ON}}{\xi}$. Here, $\lambda_M = \lambda_{Mig1p} \times \theta_M$ and $\lambda_G = \lambda_{Gal4p} \times \theta_G$.

The probabilities, θ_M and θ_G , for the binding of small molecules such as glucose and galactose to the Mig1p and Gal3p can be obtained by considering their binding partition functions.

$$\xi_M = 1 + q_{Mig} \lambda_{glu} + q_{Tup} \lambda_{Tup} q_{Mig} \lambda_{glu} \quad (S9)$$

and

$$\xi_G = 1 + q_{Gal3} \lambda_{gal} + q_{Gal80} \lambda_{gal80} q_{Gal3} \lambda_{gal} \quad (S10)$$

Here, q_{Mig} is the site partition function for the binding of glucose on Mig1p, and q_{Tup} is the site partition function for the binding of Tup1p on Mig1p. q_{Gal3} is the site partition function for the binding of galactose on Gal3p, and q_{Gal80} is the site partition function for the binding of Gal80p(that has bound to Gal4p) on Gal3p.

Also, λ_{glu} , λ_{gal} and λ_{gal80p} represent the respective activities for glucose, galactose, and gal80 protein that has bound to Gal4 protein. The probabilities, θ_M and θ_G as represented as follows.

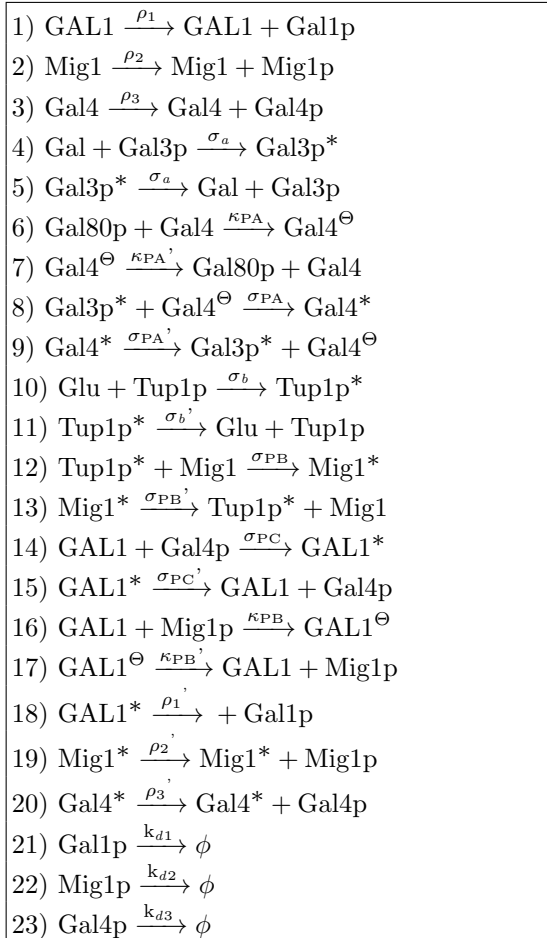
$$\theta_M = \frac{q_{Tup} \lambda_{Tup} q_{Mig} \lambda_{glu}}{\xi_M}$$

$$\theta_G = \frac{q_{Gal80} \lambda_{gal80} q_{Gal3} \lambda_{gal}}{\xi_G} \quad (S11)$$

B. Kinetic Model for a Gal promoter in a yeast cell

We further explore the dynamics of the Gal promoter regulation in the yeast cell. Specifically, we explore the effect of glucose: galactose ratio sensing in Gal promoter in a yeast cell. We present the results in the S19 and S20. It is clear from these figures that a higher quantity of glucose is not a sufficient condition for setting the GAL-responsive genes off. Instead, the ratio of glucose to galactose decides the cell fate in a yeast cell by choosing the correct form of sugar as its food source. Thus, a more significant amount of glucose and a smaller amount of galactose set the GAL-responsive genes off. Higher values of both galactose and glucose again switch on the GAL-responsive genes to some extent, which supports the quantitative prediction of ratio sense.

TABLE S10: This table contains various elementary reactions for the bio-molecular network of a yeast cell. Here, $GAL1$, $Mig1$ and $Gal4$ represent the genes with the basal expression, $GAL1^*$, $Mig1^*$ and $Gal4^*$ represent the activated genes, and $GAL1^\ominus$, $Gal4^\ominus$ represent the repressed gene. Also, $Gal1p$, $Mig1p$ and $Gal4p$ represent the proteins that are expressed by $GAL1$, $Mig1$ and $Gal4$ respectively. The specific reaction rates for each reaction are shown on the marked arrows.



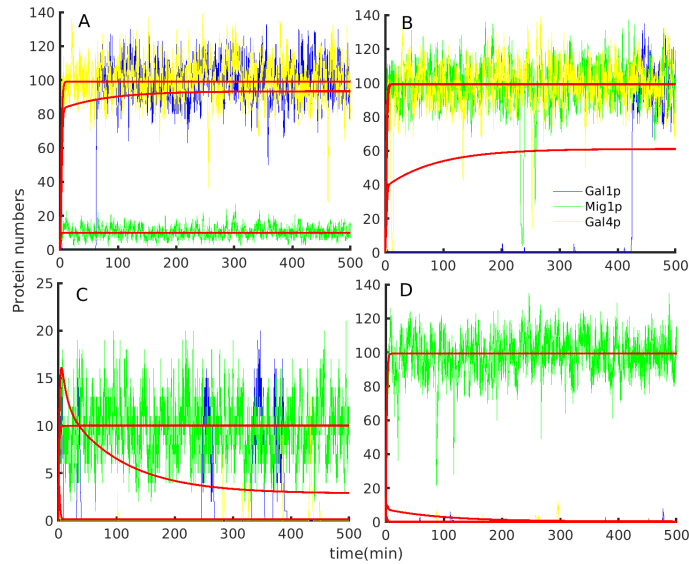


FIG. S19: Trajectories obtained from stochastic simulations are presented. Here panels A, B, C, and D refer to the presence of galactose and absence of glucose, presence of both glucose and galactose, absence of glucose and galactose, and absence of galactose and presence of glucose, respectively. Here red colored solid lines for all the cases correspond to the deterministic results. A clear correspondence between deterministic and stochastic results is visible in the figure. The parameters associated with these results are given in the table S9.

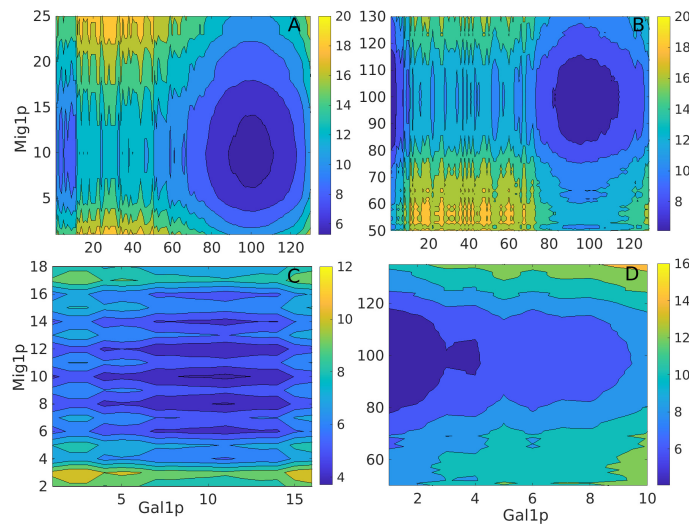


FIG. S20: The stochastic potentials for various different values of glucose and galactose for a gal promoter in a yeast cell are shown in the 2d contour maps. Here panels A, B, C, and D refer to the presence of galactose and absence of glucose, presence of both glucose and galactose, absence of glucose and galactose, and absence of galactose and presence of glucose, respectively. The parameters associated with these results are given in the table S9.

-
- [1] Hill, T. L. (1986) An introduction to statistical thermodynamics, Courier Corporation, .
 [2] Gautam, P. and Kumar Sinha, S. (2021) Anticipating response function in gene regulatory networks. *Journal of the Royal Society Interface*, **18**(179), 20210206.
 [3] Landman, J., Brewster, R. C., Weinert, F. M., Phillips, R., and Kegel, W. K. (2017) Self-consistent theory of transcriptional control in complex regulatory architectures. *PloS one*, **12**(7), e0179235.
 [4] Buchler, N. E., Gerland, U., and Hwa, T. (2003) On schemes of combinatorial transcription logic. *Proceedings of the National Academy of Sciences*, **100**(9), 5136–5141.

- [5] Einav, T., Duque, J., and Phillips, R. (2018) Theoretical analysis of inducer and operator binding for cyclic-AMP receptor protein mutants. *PloS one*, **13**(9), e0204275.
- [6] Cao, Z. and Grima, R. (2018) Linear mapping approximation of gene regulatory networks with stochastic dynamics. *Nature communications*, **9**(1), 1–15.
- [7] Cao, Z. and Grima, R. (2020) Analytical distributions for detailed models of stochastic gene expression in eukaryotic cells. *Proceedings of the National Academy of Sciences*, **117**(9), 4682–4692.
- [8] Cao, Z., Filatova, T., Oyarzún, D. A., and Grima, R. (2020) A stochastic model of gene expression with polymerase recruitment and pause release. *Biophysical Journal*, **119**(5), 1002–1014.
- [9] Venturelli, O. S., El-Samad, H., and Murray, R. M. (2012) Synergistic dual positive feedback loops established by molecular sequestration generate robust bimodal response. *Proceedings of the National Academy of Sciences*, **109**(48), E3324–E3333.
- [10] Hsu, C., Scherrer, S., Buetti-Dinh, A., Ratna, P., Pizzolato, J., Jaquet, V., and Becskei, A. (2012) Stochastic signalling rewires the interaction map of a multiple feedback network during yeast evolution. *Nature communications*, **3**(1), 682.
- [11] Kuttykrishnan, S., Sabina, J., Langton, L. L., Johnston, M., and Brent, M. R. (2010) A quantitative model of glucose signaling in yeast reveals an incoherent feed forward loop leading to a specific, transient pulse of transcription. *Proceedings of the National Academy of Sciences*, **107**(38), 16743–16748.
- [12] Peng, B., Bandari, N. C., Lu, Z., Howard, C. B., Scott, C., Trau, M., Dumsday, G., and Vickers, C. E. (2022) Engineering eukaryote-like regulatory circuits to expand artificial control mechanisms for metabolic engineering in *Saccharomyces cerevisiae*. *Communications Biology*, **5**(1), 135.
- [13] Ricci-Tam, C., Ben-Zion, I., Wang, J., Palme, J., Li, A., Savir, Y., and Springer, M. (2021) Decoupling transcription factor expression and activity enables dimmer switch gene regulation. *Science*, **372**(6539), 292–295.
- [14] Escalante-Chong, R., Savir, Y., Carroll, S. M., Ingraham, J. B., Wang, J., Marx, C. J., and Springer, M. (2015) Galactose metabolic genes in yeast respond to a ratio of galactose and glucose. *Proceedings of the National Academy of Sciences*, **112**(5), 1636–1641.